The Annals of Probability
2019, Vol. 47, No. 6, 4137–4194
https://doi.org/10.1214/19-AOP1356

A STOCHASTIC TELEGRAPH EQUATION FROM THE SIX-VERTEX MODEL[1]

BY ALEXEI BORODIN[2] AND VADIM GORIN[3]

Massachusetts Institute of Technology and Institute for Information Transmission Problems

A stochastic telegraph equation is defined by adding a random inhomogeneity to the classical (second-order linear hyperbolic) telegraph differential equation. The inhomogeneities we consider are proportional to the two-dimensional white noise, and solutions to our equation are two-dimensional random Gaussian fields. We show that such fields arise naturally as asymptotic fluctuations of the height function in a certain limit regime of the stochastic six-vertex model in a quadrant. The corresponding law of large numbers—the limit shape of the height function—is described by the (deterministic) homogeneous telegraph equation.

1. Introduction.

1.1. *Preface.* The central object of this work is a second-order inhomogeneous linear differential equation

$$f_{XY}(X,Y)+\beta_1 f_Y(X,Y)+\beta_2 f_X(X,Y)=u(X,Y),\qquad x,y\geq 0, \tag{1}$$

on an unknown function $f(X,Y)$ with given right-hand side $u(X,Y)$ and constants $\beta_1,\beta_2\in\mathbb{R}$. The equation (1) is known (in equivalent forms obtained by multiplying the unknown function f with $\exp(aX+bY)$) as the telegraph equation or the Klein–Gordon equation.

We will be particularly interested in the case when the inhomogeneity $u(X,Y)$ is proportional to the two-dimensional white noise η,

$$u(X,Y)=v(X,Y)\eta, \tag{2}$$

where the prefactor $v(X,Y)$ will be made explicit later. We call (1), (2) the *stochastic telegraph equation*.

The deterministic equation (1) is a classical object (see, e.g., [28], Chapter V) and its stochastic versions were intensively studied in the last 50 years. Random

Received July 2018; revised February 2019.

[1]Supported in part by the NSF Grant DMS-1664619.
[2]Supported in part by NSF Grant DMS-1607901.
[3]Supported in part by the NEC Corporation Fund for Research in Computers and Communications and by the Sloan Research Fellowship.
MSC2010 subject classifications. 60G60, 60H15, 35R60, 82B20.
Key words and phrases. Six-vertex model, telegraph equation, Gaussian fields.

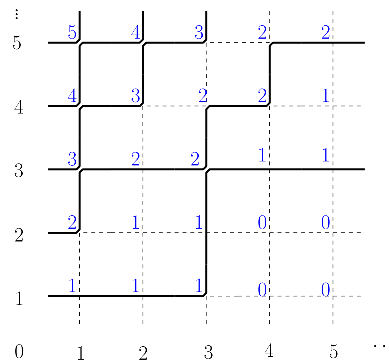

FIG. 1. *Configuration of the six-vertex model in the positive quadrant with the domain wall boundary conditions and the corresponding height function* $H(x, y)$.

terms were first added to hyperbolic PDEs in [17, 18], and there have been numerous developments since then. We will not try to survey those, but let us still mention a few. The maximum of the solution was analyzed in [53]. The existence, uniqueness and regularity of the solutions in nonlinear situations are discussed in [19, 20, 39, 50, 51, 59]. The higher-dimensional setting is considered in several articles including [22, 31, 32, 49, 52]. Significant amount of work was devoted to the design of discrete approximation schemes and numeric algorithms, for example, in [47, 48, 56, 63]. Further, [34] develops Feynman–Kac-type formulas, [33] and [23] study intermittency of the solutions, and [46] deals with (non-Gaussian) Lévy noises. Stochastic hyperbolic partial differential equations were also surveyed in [30], and mentioned in textbooks [29, 62].

The direction we take in the present paper appears different from any of the prior works, however. Our interest in the stochastic telegraph equation stems from the fact that it governs the asymptotics of the macroscopic fluctuations for a particular case of a celebrated lattice model of Statistical Mechanics called the six-vertex model; we refer to [6] for general information about this and related models.

More concretely, we deal with the *stochastic six-vertex model* (as well as its deformation—the *dynamic* six-vertex model) that was first introduced in [41] and whose asymptotic behavior has been recently studied in [1, 2, 5, 12, 25, 27, 58]. The model is defined in the positive quadrant via a sequential stochastic procedure. We postpone the exact definition till the next subsection, and for now let us just say that the configurations of the model can be viewed as collections of lattice paths on the square grid that may touch each other but can never cross; see Figure 1. These paths are further interpreted as level lines of a function $H(X, Y)$ called the *the height function*.

We investigate the limit regime in which the mesh size of the grid goes to 0, and simultaneously the turns of the paths become rare—the weights of two of the six possible local edge configurations around a vertex converge to zero. We find that the exponential $q^{H(X,Y)}$, where q is a quantization parameter involved in the definition of the model (that tends to 1 in our limit regime), converges to a nonrandom *limit shape*, which solves (1) with zero right-hand side $u(X, Y) \equiv 0$. Simultaneously, centered and scaled fluctuations of $q^{H(X,Y)}$ converge to solutions of the stochastic telegraph equation (1), (2).

The stochastic six-vertex model and our results can be put in several contexts. The asymptotic results of [12, 25, 27, 41] treat the model as an interacting particle system in the Kardar–Parisi–Zhang (KPZ) universality class [24, 44]. In fact, there is a limit transition [1, 12] from the stochastic six-vertex model to a ubiquitous member of this class—the Asymmetric Simple Exclusion Process (ASEP). There are two further limits from the ASEP to stochastic partial differential equations: the first one leads to a certain Gaussian field of fluctuations [35, 36], while the second one leads to the KPZ equation itself [4, 7, 14, 60]. However, in both cases the resulting SPDEs are stochastic versions of a *parabolic* PDE—the heat equation, while in our limit regime we observe a *hyperbolic* PDE with a stochastic term.

While the heat equation is closely related to Markov processes (indeed, the transition probabilities of the Brownian motion are given by the heat kernel), the telegraph equation (1) is not. It provides the simplest instance of a non-Markovian evolution, and we refer to [37] for a review of its relevance in physics. From the point of view of the approximation by the six-vertex model, the lack of Markov property is a corollary of the fact that for a rarely turning path, it is important to know not only its position, but also the direction in which it currently moves. Thus, in order to create a Markov process, one would need to extend the state space so that the direction is also recorded; see [55] for nice lectures about such *random evolutions*.

For the six-vertex model with fixed (i.e., not changing with the mesh size) weights, there is a general belief that the model should develop deterministic limit shapes as the mesh size goes to zero; see [54, 57]. However, mathematical understanding or description of them remains a major open problem. For special points in the space of parameters, the model is equivalent to dimer models, where the limit shape phenomenon is well understood; see [21, 45]. The approach that one uses in these cases is to develop *variational principles*, identifying limit shapes with maximizers of a certain integral functional of the slope of the shape. As a corollary, the limit shape solves Euler–Lagrange equations for the variational problem, and these equations ordinarily are *elliptic*. From this perspective, our hyperbolic PDE (1) seems difficult to predict.

In the stochastic case of the six-vertex model with fixed weights [12] computes the limit shape for the domain wall boundary conditions, and [41, 58] explain that, more generally, the limit shape has to satisfy a version of the inviscid Burgers equation. The telegraph equation can be treated as a regularization of this equation (cf. inviscid vs. viscous Burgers equation); in Remark 5.3 below, we explain how the PDE of [58] can be recovered as a limit of (1). One might be surprised that while the six-vertex hydrodynamic equation of [41, 58] does not look linear, (1) is. The explanation lies in the change of the unknown function $H(X, Y) \mapsto q^{H(X,Y)}$, which linearizes the equation. A vague analogy would be with the Hopf–Cole transform, which identifies the exponentials of solutions of the (nonlinear) KPZ equation with solutions of the (linear, with multiplicative noise) stochastic heat equation.

The same observable $q^{H(X,Y)}$ plays an important role in [25], where a convergence of the stochastic six-vertex model to the KPZ equation is proven via SPDE techniques (a one-point distributional convergence in a similar limit regime was proved in [14], Theorem 12.3, via a free fermionic reduction of [10], and a SPDE convergence in a low-density regime for higher spin stochastic vertex models was previously proved in [27]; see the introduction to [25] for a more complete bibliography of related works). The limit regime of [25] is similar to ours in the part that both address the case of *weak asymmetry* in the stochastic six-vertex model, yet the two regimes yield very different limiting SPDEs. It would be interesting to try to find an interpolation between our results and those of [25].

In the rest of the Introduction, we give a precise definition of the stochastic six-vertex model, describe our limit regime and list the asymptotic results. We further outline our results on the telegraph equation and its discrete version that, to our best knowledge, appear to be new.

1.2. *The dynamic stochastic six-vertex model.* Our main object of study is the homogeneous stochastic six-vertex model of [12, 41] and its one-parameter deformation introduced as the *dynamic stochastic six-vertex model* in [9]. Consider the configurations of the six-vertex model in positive quadrant. These are nonintersecting paths that are allowed to touch (see Figure 1) or, equivalently, assignments of six types of vertices (see Figure 3) to the integer points of the quadrant.

For some of our results, we focus on the domain wall boundary conditions, when the paths enter the quadrant through every point of its left boundary; see Figure 1. For other results, we allow arbitrary deterministic boundary conditions (configurations of incoming paths) along the x and y axes.

A key tool of our approach is the height function $H(x, y)$. It has a local definition: We set $H(1, 0) = 0$, declare that the height function is increased by 1, $H(x, y+1) - H(x, y) = 1$, whenever we move up and the segment $[(x - \frac{1}{2}, y + \frac{1}{2}), (x - \frac{1}{2}, y + \frac{3}{2})]$ crosses a path, and it is decreased by 1, $H(x+1, y) - H(x, y) = -1$, whenever we move to the right and the segment $[(x - \frac{1}{2}, y + \frac{1}{2}), (x + \frac{1}{2}, y + \frac{1}{2})]$ crosses a path. The height function is constant in regions with no paths. One way to think about the height function is that it is defined not at the integer points, but at the half-integers—centers of the faces of the square grid; then $H(x, y)$ corresponds to the point $(x - \frac{1}{2}, y + \frac{1}{2})$.[4] Figure 1 shows an example. For the domain wall boundary conditions, $H(x, y)$ counts the number of paths that pass through

[4]There is a slight asymmetry between x and y coordinates which we keep to match the notation to those of previous works.

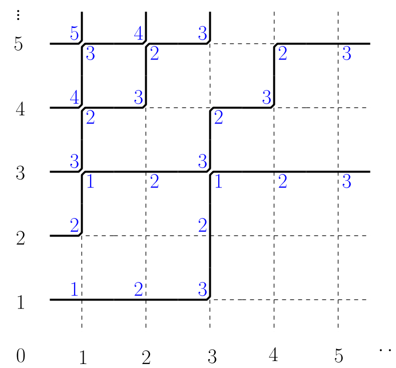

FIG. 2. *The function $d(x, y)$ defined along the paths in the dynamic stochastic six-vertex model.*

or below (x, y). Formally, for $(x, y) \in \mathbb{Z}^2_{\geq 1}$, $H(x, y)$ is the total number of vertices of types *II*, *III* and *V* at positions (x, y') with $y' \leq y$. We further extend $H(x, y)$ to real (x, y) first linearly in the x-direction, and then linearly in the y-direction. The resulting function is monotone and 1-Lipschitz in x and y directions.

We also need a modified version of the height function defined through

$$d(x, y) = x - y - 1 + 2H(x, y). \tag{3}$$

When we move one step to the right, $d(x, y)$ increases by 1 if we follow a path. When we move one step up, it *decreases* by 1 if we follow a path. Therefore, along each path the height changes piecewise-linearly, growing along the horizontal segments and decaying along the vertical ones. Note that this rule is contradictory at points where two paths touch, as we will have two values of $d(x, y)$ with difference 2; cf. Figure 2. However, this is not important, as we will never need the value of the function $d(x, y)$ at such points.

We now define the probability distribution on our path configurations. The random configuration is obtained by a sequential construction from the bottom-left corner in the upright direction, and the vertices are sampled according to the probabilities in Figure 3. The probabilities depend on three fixed real parameters: $q > 0$, $\alpha \geq 0$, $0 < b < 1$. The parameter α is sometimes referred to as the *dynamic parameter*, according to the fact that for $\alpha \neq 0$ the weights of the model satisfy the *dynamic*, or *face* variant of the Yang–Baxter equation rather than the simpler vertex one. Following the conventional terminology of statistical physics, our probability distribution can be viewed as a stochastic (or Markovian) version of a two-dimensional exactly solvable IRF (Interaction-Round-a-Face) or SOS (Solid-On-Solid) model; cf. [9]. At $\alpha = 0$, we return to the setting of the stochastic six-vertex model of [12] with $b_1 = b$, $b_2 = bq$.

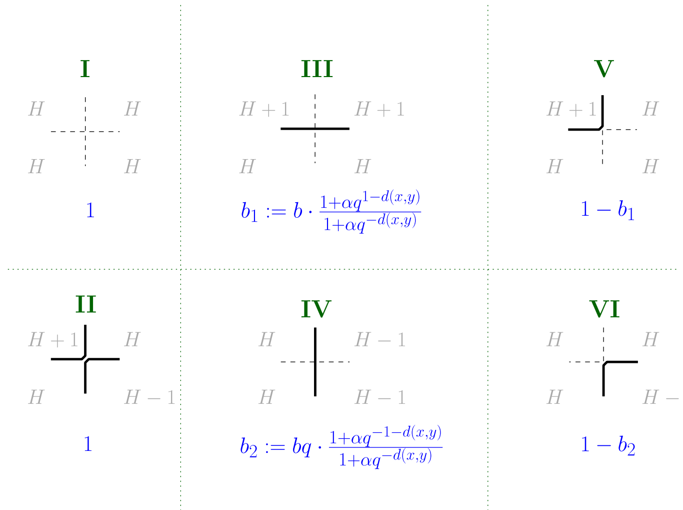

FIG. 3. *Weights of six types of vertices. Local changes of the height function $H(x, y)$ are shown in gray.*

1.3. *Limit regime and main asymptotic results.* In what follows, we take L as a large parameter and set

$$b = \exp\left(-\frac{\beta_1}{L}\right), \qquad qb = \exp\left(-\frac{\beta_2}{L}\right), \qquad \beta_1, \beta_2 > 0, \beta_1 \neq \beta_2. \tag{4}$$

The parameter $\alpha \geq 0$ will remain fixed. In particular, if $\alpha = 0$, then

$$b_1 = \exp\left(-\frac{\beta_1}{L}\right), \qquad b_2 = \exp\left(-\frac{\beta_2}{L}\right).$$

Further, we consider the limit $L \to \infty$, and it is sometimes convenient to use alternative parameters $\mathfrak{q}$ and $\mathfrak{s}$ defined by

$$q = \mathfrak{q}^{1/L}, \qquad \ln(\mathfrak{q}) = \beta_1 - \beta_2, \qquad \mathfrak{s} = \lim_{L\to\infty} \frac{1-b}{1-bq} = \frac{\beta_1}{\beta_2}. \tag{5}$$

We will sometimes switch between β_1, β_2 notation and $\mathfrak{q}$, $\mathfrak{s}$ notation to make formulas more aesthetically pleasing. We will always assume $\beta_1 \neq \beta_2$, which implies $\mathfrak{q}, \mathfrak{s} \neq 1$.

We prove the following results:

1. For the domain wall boundary conditions and any $\alpha \geq 0$, we develop in Theorems 2.1, 2.4 the law of large numbers for the height function $H(x, y)$ and the central limit theorem for its centered and rescaled fluctuations. The relevant limit quantities are given as contour integrals, and the proofs are based on exact expressions for the expectation of shifted q-moments of the height function $H(X, Y)$.

We rely on several ingredients—contour integral expressions of [9], a Gaussianity lemma for random variables with moments given by contour integrals of [13], and a novel combinatorial argument of Theorem 2.10 linking cumulants with their shifted versions.

2. For *arbitrary* (deterministic) boundary conditions in the case $\alpha = 0$, we prove in Theorem 5.1 the law of large numbers by showing that $q^{H(x,y)}$ converges in probability to the solution of the telegraph equation (1) with $u(x, y) \equiv 0$ and prescribed boundary values along the lines $x = 0$ and $y = 0$. The proof is based on a novel stochastic four-point relation of Theorem 3.1 for $q^{H(x,y)}$. This relation does not seem to be present in the existing literature but, once written, its proof is immediate from the definition of the model. It can also be derived from the duality relations of [26], (2.6), [27], Proposition 2.6, [25], Corollary 3.4. We were led to this relation by [64] that provided different derivations of its averaged version.

3. For *arbitrary* (deterministic) boundary conditions in the $\alpha = 0$ case, we present the central limit theorem for $q^{H(x,y)}$ in Theorem 6.1. The answer is given by the stochastic telegraph equation (1), (2) with the variance of the white noise $v(x, y)$ being a *nonlinear* function of the limiting profile for $q^{H(x,y)}$ afforded by the law of large numbers. The proof again exploits the four-point relation of Theorem 3.1.

4. We investigate the *low density* boundary conditions (which means that there are few paths entering through the boundary; their locations are still deterministic, but they are changing as $L \to \infty$; the distinction with previous results is that in points 2 and 3 the average density of incoming paths was positive, while here it tends to 0), in the case $\alpha = 0$, which has an interpretation through evolution of a family of independent persistent random walks. We prove in Theorem 7.1 the law of large numbers and central limit theorem for the properly centered and scaled $H(x, y)$. The answer is still given by the stochastic telegraph equation (1), (2), but the variance of the white noise $v(x, y)$ becomes a *linear* function of the limiting profile.

In the first version of this text the central limit theorem of (3) was presented as a conjecture with two heuristic arguments in favor of its validity. Later on, [61] proved the conjecture by combining the four-point relation with certain new ideas. This prompted us to return to our original heuristic approaches, and we were eventually able to turn one of them into a complete proof (different from the one in [61]). It is this proof that is presented in Section 6 below; the second heuristic approach has been moved to an Appendix.

1.4. *The classical telegraph equation and its discretization.* As many of our results are based on the analysis of the telegraph equation (1) and its discrete counterpart encoded in the four-point relation of Theorem 3.1, we need some information about its solutions. There is a classical part here (see, e.g., [28])—existence/uniqueness of the solutions to hyperbolic PDEs and an integral representation of the solutions through the *Riemann function* of the equation. We review

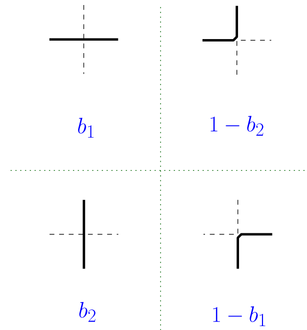

FIG. 4. *The weights of the random walk toward the origin.*

this part at the beginning of Section 4. We further demonstrate in Theorem 4.7 that the discrete version of the telegraph equation admits a similar theory, with the Riemann function replaced by an appropriate discrete analogue. This greatly simplifies the proofs, as the convergence of the discretization to the telegraph equation itself becomes a corollary of the convergence for the (explicit) Riemann functions.

Motivated by the fact that we obtained the telegraph equation from a stochastic system of nonintersecting paths, we further develop a theory for the representations of its solutions as path integrals. This may be viewed as an analogue of the Feynman–Kac formula for the parabolic equations. For the homogeneous equation (1) with $u(x, y) \equiv 0$, such a theory was previously known—[40, 43] (see also [55]), explain that a solution at (x, y) can be represented as an expectation of the boundary data at the point where a *persistent Poisson random walk* started at (x, y) exits the quadrant; see Theorem 4.11 for the exact statement.

For the inhomogeneous equation, we find a stochastic representation (that we have not seen before) in terms of *two* persistent Poisson random walks. The additional term is the integral of the right-hand side $u(X, Y)$ over the domain between two (random) paths with sign depending on which path is higher. We refer to Theorem 4.11 for more details.

In addition, we develop, in Theorems 4.8, 4.9, a stochastic representation for the solutions of the discretization of the telegraph equation. The result is similar: one needs to launch a random walk from the observation point and compute the expectation at the exit point to get the influence of the boundary data, and one needs to sum the inhomogeneity of the equation over the domain between trajectories of two random walks. The needed random walk combinatorially is the same path of the six-vertex model, but with flipped stochastic weights, as in Figure 4.

2. The domain wall boundary conditions. In this section, we focus on the domain wall boundary conditions: the paths enter at every integer point of the y-axis and no paths enter through the x-axis, as in Figures 1, 2. We prove the law of large numbers and the central limit theorem for the height function.

2.1. *Formulation of LLN and CLT.*

THEOREM 2.1. *For each $\alpha \geq 0$, in the limit regime* (4) *we have*

$$\lim_{L\to\infty} \frac{1}{L} H(Lx, Ly) = \mathbf{h}(x, y) \quad (\textit{convergence in probability}),$$

where $\mathbf{h}(x, y)$ is the only real (*deterministic*) *solution of*

$$\begin{aligned}&\frac{(\mathfrak{q}^{-\mathbf{h}(x,y)}\mathfrak{q}^{y-x} + \alpha^{-1})(\mathfrak{q}^{\mathbf{h}(x,y)} - 1)}{1 + \alpha^{-1}} \\ &\quad = \frac{1}{2\pi \mathbf{i}} \oint_{-1} \exp\Big(\ln(\mathfrak{q})\Big(-x\frac{\mathfrak{s}z}{1+\mathfrak{s}z} + y\frac{z}{1+z}\Big)\Big)\frac{dz}{z},\end{aligned} \tag{6}$$

with integration in positive direction around the singularity at -1 and avoiding the singularities at 0 and $-\frac{1}{\mathfrak{s}}$. At $\alpha = 0$, the left-hand side of (6) *becomes $\mathfrak{q}^{\mathbf{h}(x,y)} - 1$.*

REMARK 2.2. In terms of β_1 and β_2, the right-hand side of (6) can be rewritten as

$$\frac{1}{2\pi \mathbf{i}} \oint_{-\beta_1} \exp\Big((\beta_1 - \beta_2)\Big(-x\frac{z}{\beta_2+z} + y\frac{z}{\beta_1+z}\Big)\Big)\frac{dz}{z} \tag{7}$$

with a positively oriented integration contour encircling $z = -\beta_1$, but not $-\beta_2$ or 0.

PROPOSITION 2.3. *In the setting of Theorem* 2.1 *with $\alpha = 0$, consider the limit $\mathfrak{q} \to 0$ with fixed value of $\mathfrak{s} < 1$. Then*

$$\lim_{\mathfrak{q}\to 0} \mathbf{h}(x, y) = \begin{cases} 0, & \dfrac{x}{y} > \mathfrak{s}^{-1}, \\ \dfrac{(\sqrt{\mathfrak{s}x} - \sqrt{y})^2}{1-\mathfrak{s}}, & \mathfrak{s} \leq \dfrac{x}{y} \leq \mathfrak{s}^{-1} \\ y - x, & \dfrac{x}{y} < \mathfrak{s}. \end{cases} \tag{8}$$

Note that the right-hand side of (8) is precisely the limit shape of the stochastic six-vertex model in the asymptotic regime of fixed q as $L \to \infty$, as obtained in [12], Theorem 1.1.

Let us apply the differential operator $f \mapsto f_{xy} + \beta_1 f_y + \beta_2 f_x$ to (7). We can differentiate under the integral sign, which gives

$$\begin{aligned}&\frac{1}{2\pi \mathbf{i}} \oint_{-\beta_1} \frac{dz}{z} \exp\Big((\beta_1 - \beta_2)\Big(-x\frac{z}{\beta_2+z} + y\frac{z}{\beta_1+z}\Big)\Big) \\ &\quad \times \Big[-(\beta_1-\beta_2)^2\frac{z}{\beta_1+z}\cdot\frac{z}{\beta_2+z} \\ &\quad + \beta_1(\beta_1-\beta_2)\frac{z}{\beta_1+z} - \beta_2(\beta_1-\beta_2)\frac{z}{\beta_2+z}\Big] = 0.\end{aligned} \tag{9}$$

This shows that a functional of the limit shape (which is $\mathfrak{q}^{\mathbf{h}(x,y)}$ in $\alpha = 0$ case and the left-hand side of (6) for general α) satisfies the equation $f_{xy} + \beta_1 f_y + \beta_2 f_x = 0$, which is a variant of the telegraph equation; cf., for example, [28]. In Section 5, we upgrade the law of large numbers at $\alpha = 0$ to general boundary conditions and prove that the link to the telegraph equation persists.

For a point $(x, y) \in \mathbb{Z}_{>0} \times \mathbb{Z}_{>0}$, define

$$\mathcal{O}(x, y) = -\alpha^{-1} q^{H(x,y)} + q^{y-x+1-H(x,y)}. \tag{10}$$

THEOREM 2.4. *Fix $k \in \mathbb{Z}_{>0}$ and reals $y > 0$ and $x_1 \geq x_2 \geq \cdots \geq x_k > 0$. For each $\alpha \geq 0$, in the limit regime (4) the random variables*

$$\frac{H(Lx_i, Ly) - \mathbb{E}H(Lx_i, Ly)}{\sqrt{L}}, \quad i = 1, \dots, k,$$

converge as $L \to \infty$ (in the sense of moments) to a centered Gaussian vector. The asymptotic covariance is given in terms of $\mathcal{O}(x, y)$ by

$$\begin{aligned}
&\lim_{L\to\infty} L \frac{\operatorname{Cov}(\mathcal{O}(Lx_1, Ly), \mathcal{O}(Lx_2, Ly))}{(1+\alpha^{-1})^2} \\
&\quad = \frac{\ln(\mathfrak{q})}{(2\pi \mathbf{i})^2} \oint_{-1} \oint_{-1} \frac{z_1}{z_1 - z_2} \prod_{i=1}^{2} \left[\exp\left(\ln(\mathfrak{q}) \left(-x_i \frac{\mathfrak{s} z_i}{1 + \mathfrak{s} z_i} + y \frac{z_i}{1 + z_i} \right) \right) \frac{dz_i}{z_i} \right] \\
&\quad + \frac{\ln(\mathfrak{q})}{2\pi \mathbf{i}} \oint_{-1} \exp\left(\ln(\mathfrak{q}) \left(-x_1 \frac{\mathfrak{s} z}{1 + \mathfrak{s} z} + y \frac{z}{1+z} \right) \right) \frac{dz}{z} \\
&\quad \times \frac{1}{1+\alpha^{-1}} \Bigg[\mathfrak{q}^{y - x_2} + \alpha^{-1} \\
&\quad + \frac{1}{2\pi \mathbf{i}} \oint_{-1} \exp\left(\ln(\mathfrak{q}) \left(-x_2 \frac{\mathfrak{s} z}{1 + \mathfrak{s} z} + y \frac{z}{1+z} \right) \right) \frac{dz}{z} \Bigg],
\end{aligned} \tag{11}$$

where $x_1 \geq x_2$, positively oriented integration contours enclose -1, but not 0 or $-\frac{1}{\mathfrak{s}}$, and for the first integral the z_1-contour is inside the z_2-contour. If $\alpha = 0$, then

$$\begin{aligned}
&\lim_{L\to\infty} L \operatorname{Cov}\left(q^{H(Lx_1, Ly)}, q^{H(Lx_2, Ly)}\right) \\
&\quad = \frac{\ln(\mathfrak{q})}{(2\pi \mathbf{i})^2} \oint_{-1} \oint_{-1} \frac{z_1}{z_1 - z_2} \prod_{i=1}^{2} \left[\exp\left(\ln(\mathfrak{q}) \left(-x_i \frac{\mathfrak{s} z_i}{1 + \mathfrak{s} z_i} + y \frac{z_i}{1 + z_i} \right) \right) \frac{dz_i}{z_i} \right] \\
&\quad + \frac{\ln(\mathfrak{q})}{2\pi \mathbf{i}} \oint_{-1} \exp\left(\ln(\mathfrak{q}) \left(-x_1 \frac{\mathfrak{s} z}{1 + \mathfrak{s} z} + y \frac{z}{1+z} \right) \right) \frac{dz}{z}, \quad x_1 \geq x_2,
\end{aligned} \tag{12}$$

with similar integration contours.

REMARK 2.5. Expanding

$$q^{H(Lx,Ly)} = q^{\mathbb{E}H(Lx,Ly)}\Big(1 + \ln(q)\big(H(Lx,Ly) - \mathbb{E}H(Lx,Ly)\big) + \big(\ln(q)\big)^2 \frac{(H(Lx,Ly) - \mathbb{E}H(Lx,Ly))^2}{L^2} + \cdots\Big),$$

and noticing that $\ln(q)$ is of order L^{-1}, one can derive the covariance of $H(Lx, Ly)$ from that of $q^{H(Lx,Ly)}$, or from that of $\mathcal{O}(Lx, Ly)$. However, the resulting formulas are much bulkier than (11), (12) and we have not found a good way to simplify them.

At $\alpha = 0$, we can generalize Theorem 2.4; in Section 6, we describe its upgrade to general boundary conditions and link it to a stochastic telegraph equation.

In the remainder of this section, we prove Theorems 2.1, 2.4 and Proposition 2.3.

2.2. *Observables*. The asymptotic analysis of this section is based on (algebraic) results from [9] that generalize those of [12, 15, 16, 26]; more powerful results can be found in [3].

As before, we use the notation $\mathcal{O}(x, y) = -\alpha^{-1} q^{H(x,y)} + q^{y-x+1-H(x,y)}$.

THEOREM 2.6 ([9], Theorem 10.1). *For any fixed $y \ge 1$ and $x_1 \ge x_2 \ge \cdots \ge x_n \in \mathbb{Z}_{>0}$, the expectation*

$$E_N(x_1, \dots, x_N) := \frac{1}{(-\alpha^{-1}; q)_n} \mathbb{E}\Bigg[\prod_{k=1}^{n} \big(q^{y-x_k+1} - \alpha^{-1} q^{2k-2} - q^{k-1}\mathcal{O}(x_k, y)\big)\Bigg] \tag{13}$$

is equal to

$$\frac{q^{n(n-1)/2}}{(2\pi \mathbf{i})^n} \oint \cdots \oint \prod_{1 \le i < j \le n} \frac{z_i - z_j}{z_i - q z_j} \times \prod_{i=1}^{n} \Bigg[\bigg(\frac{1 + q^{-1}\frac{1-b}{1-qb} z_i}{1 + \frac{1-b}{1-qb} z_i}\bigg)^{x_i - 1} \bigg(\frac{1 + z_i}{1 + q^{-1} z_i}\bigg)^{y} \frac{dz_i}{z_i}\Bigg], \tag{14}$$

with positively oriented integration contours encircling $-q$ and no other poles of the integrand. In particular, $E_N(x_1, \dots, x_N)$ does not depend on α.

REMARK 2.7. The expression $q^{y-x+1} - \alpha^{-1} q^{2k-2} - q^{k-1}\mathcal{O}(x, y)$ in (13) can be written as

$$\big(q^{y-x+1} q^{-H(x,y)} + \alpha^{-1} q^{k-1}\big)\big(q^{H(x,y)} - q^{k-1}\big).$$

In the case $\alpha = 0$, the observable E_N simplifies to

$$E_N(x_1, \dots, x_N)|_{\alpha=0} = \mathbb{E}\Bigg[\prod_{k=1}^{n} \big(q^{H(x_k,y)} - q^{k-1}\big)\Bigg]. \tag{15}$$

REMARK 2.8. The formula (14) matches [12], Theorem 4.12, with $x_1 = x_2 = \cdots = t + 1$, $y = x$. Note that there is a shift by 1 because of slightly different coordinate systems.

PROPOSITION 2.9. *In* (14), *for each* $n \geq 1$, *and for* q, b *sufficiently close to* 1, *one can deform the contours so that they still include the poles at* $-q$, *and in addition are nested*: z_i *is inside* qz_j *for* $1 \leq i < j \leq n$. *This deformation does not change the value of the integral.*

We omit the proof of Proposition 2.9, as it is a direct contour deformation similar to [16], Theorem 8.13; see also discussion after Proposition 2.2 in [10]. In what follows, we always use the result of Theorem 2.6 on the contours of Proposition 2.9.

2.3. *Limit of expectation.* Straightforward limit transition in the $N = 1$ version of Theorem 2.6 yields that

$$\lim_{L\to\infty} \mathbb{E}\left[\frac{\mathfrak{q}^{y-x} - \alpha^{-1} - \mathcal{O}(Lx, Ly)}{1 - \alpha^{-1}}\right]$$

is the expression in the right-hand side of (6).

Second-order expansion of $N = 1$ version of Theorem 2.6 can be similarly used to obtain the second-order expansion of $\mathbb{E}[\mathcal{O}(Lx, Ly)]$ as $L \to \infty$. This expectation is used for the centering in Theorem 2.4.

2.4. *Limit of covariance.* Applying $N = 2$ version of Theorem 2.6, we get for $x_1 \geq x_2$,

$$\begin{aligned}
&\lim_{L\to\infty} L\big[E_2(Lx_1, Lx_2) - E_1(Lx_1)E_1(Lx_2)\big] \\
&\quad= \frac{L}{(2\pi\mathbf{i})^2} \oint\oint \left[\frac{qz_1 - qz_2}{z_1 - qz_2} - 1\right] \\
&\qquad\times \prod_{i=1}^{2}\left[\left(\frac{1 + q^{-1}\frac{1-b}{1-qb}z_i}{1 + \frac{1-b}{1-qb}z_i}\right)^{x_i - 1}\left(\frac{1 + z_i}{1 + q^{-1}z_i}\right)^{y}\frac{dz_i}{z_i}\right] \\
&\quad= \frac{\ln(\mathfrak{q})}{(2\pi\mathbf{i})^2} \oint\oint \frac{z_1}{z_1 - z_2} \prod_{i=1}^{2}\left[\exp\left(\ln(\mathfrak{q})\left(-x_i\frac{\mathfrak{s}z_i}{1 + \mathfrak{s}z_i} + y\frac{z_i}{1 + z_i}\right)\right)\frac{dz_i}{z_i}\right],
\end{aligned} \tag{16}$$

where the contours (see Proposition 2.9) are such that they both enclose -1 and z_1-contour is inside the z_2-contour. On the other hand,

$$\begin{aligned} & E_2(Lx_1, Lx_2) \\ & \quad = \frac{1}{(1+\alpha^{-1})(1+\alpha^{-1}q)}\mathbb{E}\Bigg[\prod_{k=1}^{2}\big(q^{Ly-Lx_k+1} - \alpha^{-1}q^{2k-2} \\ & \qquad - q^{k-1}\mathbb{E}\mathcal{O}(Lx_k, Ly) - q^{k-1}\big(\mathcal{O}(Lx_k, Ly) - \mathbb{E}\mathcal{O}(Lx_k, Ly)\big)\big)\Bigg] \\ & \quad = \frac{\prod_{k=1}^{2}\mathbb{E}[q^{Ly-Lx_k+1} - \alpha^{-1}q^{2k-2} - q^{k-1}\mathcal{O}(Lx_k, Ly)]}{(1+\alpha^{-1})(1+\alpha^{-1}q)} \\ & \qquad + \frac{q\,\mathrm{Cov}(\mathcal{O}(Lx_1, Ly), \mathcal{O}(Lx_2, Ly))}{(1+\alpha^{-1})(1+q\alpha^{-1})}. \end{aligned} \tag{17}$$

Thus, as $L \to \infty$ in the regime (4),

$$\begin{aligned} & E_2(Lx_1, Lx_2) - E_1(Lx_1)E_1(Lx_2) \\ & \quad = \frac{q\,\mathrm{Cov}(\mathcal{O}(Lx_1, Ly), \mathcal{O}(Lx_2, Ly))}{(1+\alpha^{-1})(1+q\alpha^{-1})} \\ & \qquad + \frac{\mathbb{E}[q^{Ly-Lx_1+1} - \alpha^{-1} - \mathcal{O}(Lx_1, Ly)]}{(1+\alpha^{-1})} \\ & \qquad \times \bigg(\frac{\mathbb{E}[q^{Ly-Lx_2+1} - \alpha^{-1}q^2 - q\mathcal{O}(Lx_2, Ly)]}{(1+q\alpha^{-1})} \\ & \qquad - \frac{\mathbb{E}[q^{Ly-Lx_2+1} - \alpha^{-1} - \mathcal{O}(Lx_2, Ly)]}{(1+\alpha^{-1})}\bigg), \end{aligned}$$

which can be transformed into

$$\begin{aligned} & \frac{q\,\mathrm{Cov}(\mathcal{O}(Lx_1, Ly), \mathcal{O}(Lx_2, Ly))}{(1+\alpha^{-1})(1+q\alpha^{-1})} + O\big((1-q)^2\big) \\ & \quad + \frac{(1-q)\alpha^{-1}\prod_{k=1}^{2}\mathbb{E}[q^{Ly-Lx_k+1} - \alpha^{-1} - \mathcal{O}(Lx_k, Ly)]}{(1+\alpha^{-1})^3} \\ & \quad + \frac{\mathbb{E}[q^{Ly-Lx_1+1} - \alpha^{-1} - \mathcal{O}(Lx_1, Ly)]}{(1+\alpha^{-1})^2} \\ & \quad \times \big(\alpha^{-1}(1-q^2) + (1-q)\mathbb{E}\mathcal{O}(Lx_2, Ly)\big). \end{aligned}$$

We conclude that

$$\lim_{L\to\infty}\frac{L\,\mathrm{Cov}(\mathcal{O}(Lx_1,Ly),\mathcal{O}(Lx_2,Ly))}{(1+\alpha^{-1})^2}$$

$$(18)\qquad = \lim_{L\to\infty} L\big[E_2(Lx_1,Lx_2)-E_1(Lx_1)E_1(Lx_2)\big]$$

$$+\ln(\mathfrak{q})\lim_{L\to\infty}\big[E_1(Lx_1)\big]\frac{\lim_{L\to\infty}[E_1(Lx_2)]+\mathfrak{q}^{y-x_2}+\alpha^{-1}}{1+\alpha^{-1}}.$$

Using (18), (16) and the computation of Section 2.3 we arrive at (11).

2.5. *Cumulant-type sums.* Our proof of the asymptotic Gaussianity in Theorem 2.4 relies on a combinatorial statement presented in this section.

Let $\mathbb{S}_n$ denote the set of all *set partitions* of $\{1,\dots,n\}$. An element $s\in\mathbb{S}_N$ is a collection $S_1,\dots,S_k$ of disjoint subsets of $\{1,\dots,n\}$ such that

$$\bigcup_{m=1}^{k} S_m=\{1,\dots,n\}.$$

The number of nonempty sets in $s\in\mathbb{S}_n$ will be called the *length* of s and denoted as $\ell(s)$.

Fix $n=1,2,\dots$ and suppose that for each subset $A\subset\{1,2,\dots,n\}$ we are given a number M_A called the "joint moment of A." Then we define the corresponding joint cumulant C_n through

$$(19)\qquad C_n:=\sum_{s\in\mathbb{S}_n}(-1)^{\ell(s)+1}\big(\ell(s)-1\big)!\prod_{A\in s}M_A.$$

THEOREM 2.10. *Fix $n>2$. Take n random variables $\xi_1,\dots,\xi_n$, n deterministic real numbers $r_1,\dots,r_n$, $n(n-1)/2$ real numbers a_{ij}, $1\le i<j\le n$, and an auxiliary small parameter $\varepsilon>0$. Define two different sets of moments M_A, M'_A for $A=\{i_1<i_2<\dots<i_m\}\subset\{1,\dots,n\}$ through*

$$(20)\quad M_A=\mathbb{E}\left[\prod_{k=1}^{m}\xi_{i_k}\right],\qquad M'_A=\mathbb{E}\left[\prod_{k=1}^{m}(r_{i_k}+\varepsilon\cdot\xi_{i_k})\right]\prod_{1\le k<l\le m}\big(1+\varepsilon^2\cdot a_{i_k,i_l}\big).$$

Then the corresponding cumulants C_n, C'_n given by (19) are related through

$$(21)\qquad \begin{aligned} C'_n&=\varepsilon^n\cdot C_n+\varepsilon^{n+1}\cdot P(\varepsilon,r_i,a_{ij},\xi_i)\quad \textit{or}\\ C_n&=\varepsilon^{-n}\cdot C'_n-\varepsilon\cdot P(\varepsilon,r_i,a_{ij},\xi_i),\end{aligned}$$

where the remainder P is a polynomial in ε, r_i, a_{ij}, $1\le i,j\le n$ and joint moments of ξ_i of the total order up to n.

REMARK 2.11. If a_{ij} depend only on the second index, $a_{i,j} = \tilde{a}_j$, then M'_A can be rewritten as

$$M'_A = \mathbb{E}\left(\prod_{k=1}^{m}\left[(r_{i_k} + \varepsilon \cdot \xi_{i_k})(1 + \varepsilon^2 \cdot \tilde{a}_{i_k})^{k-1}\right]\right). \tag{22}$$

This is the form which appears in our proof of Theorem 2.4.

PROOF OF THEOREM 2.10. Let us expand M'_A into a large sum, opening the parentheses, substitute into C'_n and collect the terms. Each term is a product of (usual) moments M_B, numbers r_{i_k} and a_{i_k,i_l}, and powers of ε. We plug in the expansions into the definition of C'_n and further expand and collect the same terms as much as possible.

Let us introduce a combinatorial encoding for each term of the resulting sum. We start with n vertices, representing the indices $\{1, 2, \dots, n\}$. We proceed by drawing edges between some of the vertices: an edge joining i with j represents the factor $\varepsilon^2 \cdot a_{i,j}$, $i < j$. Some of the vertices will be linked into (disjoint) clusters: a cluster with vertices $i_1, \dots, i_m$ represents the factor $\varepsilon^m \mathbb{E}[\prod_{k=1}^m \xi_{i_k}]$. Any vertex t that does not belong to any cluster produces the factor r_t. We call the resulting combinatorial structure a clustered graph and identify it with the expression obtained by multiplying the factors corresponding to its edges and clusters.

Claim. For each clustered graph with nonzero contribution to C'_n, one of the following holds:

1. Either there are no clusters and the remaining graph is connected,
or
2. Each vertex is connected (by a path consisting of edges) to a vertex belonging to a cluster (in other words, each edge-connected component intersects with a cluster).

Putting it otherwise, the claim says that if we fix a clustered graph for which neither of the conditions holds, then the sum of the terms in C'_n corresponding to this graph vanishes. Before proving the claim note that it implies the statement of the theorem. Indeed, if there are no clusters, then we must have at least $n-1$ edges, which produces the factor $\varepsilon^{2(n-1)} = O(\varepsilon^{n+1})$. Otherwise, each vertex in a cluster produces a factor of ε, and all vertices outside the clusters produce at least ε^{m+1}, where $m \geq 1$ is their number. Altogether we again get $O(\varepsilon^{n+1})$. We conclude that the only structures that have the power of ε smaller than ε^{n+1} are those with no edges at all and with all vertices belonging to some clusters. This gives ε^n prefactor and these terms precisely combine into the conventional cumulant C_n.

We now prove the claim. Fix a clustered graph G for which neither of the properties hold. Then this graph has an edge-connected component A which does not intersect with clusters and $A \neq \{1, \dots, n\}$. Take a set partition s_0 of the set $\{1, \dots, n\} \setminus A$. Note that each set partition s in (19) for which the graph G arises in the decomposition (when M_A are replaced by M'_A), is necessarily obtained by taking such s_0 and then either adding A to one of the sets, or by putting A as a new set of the partition. Each choice leads to one appearance of G. Let us sum over all these choices. For that, suppose that s_0 has r parts. When we add A to one of the sets of s_0, then the resulting partition has r parts and, therefore, the corresponding coefficient in (19) is $(-1)^{r+1}(r-1)!$. On the other hand, if A creates a new set, then the coefficient becomes $(-1)^{r+2}r!$. Since there are precisely r sets to which A can be added and $r\cdot(-1)^{r+1}(r-1)!+(-1)^{r+2}r!=0$, we see that the total contribution of G in (19) (with M'_A instead of M_A) vanishes. □

2.6. *Proof of LLN and CLT.*

PROOF OF THEOREM 2.1. In Section 2.3, we have shown that $\mathbb{E}(\mathcal{O}(Lx,Ly))$ converges to the expression given by (6). The covariance computation of Section 2.4 implies that $\lim_{L\to\infty}\mathbb{E}(\mathcal{O}(Lx,Ly)-\mathbb{E}(\mathcal{O}(Lx,Ly)))^2=0$ and, therefore, $\mathcal{O}(Lx,Ly)$ converges in probability to the deterministic limit given by (6). Since $\frac{1}{L}H(Lx,Ly)$ is obtained from $\mathcal{O}(Lx,Ly)$ by applying a strictly monotone uniformly Lipschitz map (cf. (10)), we deduce the convergence for $\frac{1}{L}H(Lx,Ly)$ as well. □

PROOF OF THEOREM 2.4. In Section 2.4, we obtained the formulas for the asymptotic covariance of $L^{1/2}\mathcal{O}(Lx_k,Ly)$ which matches (11), (12). It remains to prove the asymptotic Gaussianity, for which we are going to show that the joint cumulants of $L^{1/2}\mathcal{O}(Lx_k,Ly)$ of orders higher than 2 vanish as $L\to\infty$.

Fix $n>3$ and take n-tuple $x_1\le x_2\le\cdots\le x_n$. We aim to prove that the nth joint cumulant of $\{\mathcal{O}(Lx_k,Ly)\}_{k=1}^n$, which we denote C_n, decays faster than $L^{-n/2}$ as $L\to\infty$.

For a set $A=\{i_1<i_2<\cdots<i_m\}\subset\{1,2,\dots,n\}$, let $M'_A=E_m(i_1,i_2,\dots,i_m)$, as given by (14). As in Section 2.5, we denote through C'_n the corresponding joint "cumulant." Contour integral expressions of Theorem 2.6 combined with [13], Lemma 4.2, (with $\gamma=1$) yields that $C'_n=o(L^{-n/2})$ as $L\to\infty$.

Note that *a priori* C'_n is different from the conventional cumulant C_n. However, we can relate them using Theorem 2.10. For that, we write

$$\mathcal{O}(Lx,Ly)=\mathcal{O}_\infty(x,y)+L^{-1/2}\Delta\mathcal{O}(x,y),$$

where $\mathcal{O}_\infty(x,y)=\mathbb{E}\mathcal{O}(Lx,Ly)$ and $\Delta\mathcal{O}(x,y)$ is the fluctuation, for which we know (from the covariance computation of Section 2.4) that it is tight as $L\to\infty$.

Then we transform $E_m(Lx_1,\dots,Lx_m)$ as

$$\begin{aligned}&\mathbb{E}\prod_{k=1}^m\frac{q^{Ly-Lx_k+1}-\alpha^{-1}q^{2k-2}-q^{k-1}\mathcal{O}(Lx_k,Ly)}{1+\alpha^{-1}q^{k-1}}\\ &\quad=\mathbb{E}\prod_{k=1}^m\frac{q^{Ly-Lx_k+1}-\alpha^{-1}q^{2(k-1)}-q^{k-1}\mathcal{O}_\infty(x_k,y)-q^{k-1}L^{-1/2}\Delta\mathcal{O}(x,y)}{(1+\alpha^{-1})(1+\frac{\alpha^{-1}}{1+\alpha^{-1}}(q^{k-1}-1))}.\end{aligned}\tag{23}$$

Let us examine the kth factor of (23). The numerator splits into four terms, each of them has the form appearing in Theorem 2.10. We need to deal with the denominator. For that, we choose an integer $M > n/2$ and expand

$$\begin{aligned}&\frac{1}{(1+\alpha^{-1})(1+\frac{\alpha^{-1}}{1+\alpha^{-1}}(q^{k-1}-1))}\\&\quad=\frac{1}{1+\alpha^{-1}}\biggl[1-\frac{\alpha^{-1}}{1+\alpha^{-1}}(q^{k-1}-1)\\&\qquad+\biggl(\frac{\alpha^{-1}}{1+\alpha^{-1}}(q^{k-1}-1)\biggr)^2+\cdots\\&\qquad+\biggl(\frac{\alpha^{-1}}{1+\alpha^{-1}}(q^{k-1}-1)\biggr)^M+o\bigl((q-1)^M\bigr)\biggr].\end{aligned}$$

Note that we can ignore $o((q-1)^M)$, as this term has smaller order than the desired cumulants. In the rest, we expand each $(q^{k-1}-1)^b$ into $b+1$ terms using the binomial theorem. Altogether we get $1+2+\cdots+(M+1)=(M+1)(M+2)/2$ terms.

We plug the resulting sum into the kth factor of (23) and get a sum of $2(M+1)(M+2)$ terms. Each term has a form

$$r\cdot\bigl[\bigl(1+(q-1)\bigr)^u\bigr]^{k-1}\quad\text{or}\quad L^{-1/2}\xi\bigl[\bigl(1+(q-1)\bigr)^u\bigr]^{k-1},$$

where u is a positive integer, r is a deterministic number, ξ is a random variable. We arrive at an expression of the form of the definition of M'_A in (20); see Remark 2.11. The conclusion is that (23) turns into a sum of finitely many expressions, each of which has the form of M'_A (for various choices of parameters) in Theorem 2.10.

At this point, we would like to apply Theorem 2.10 with $\varepsilon = L^{-1/2}$. Note that the "cumulants" C'_n in this theorem are multilinear over the choices of r_i and ξ_i. In other words, if we fix $1 \le t \le n$, set $r_t = r_t[1] + r_t[2]$, $\xi_t = \xi_t[1] + \xi_t[2]$ and denote the resulting cumulants through $C'_n[1]$, $C'_n[2]$, then $C'_n = C'_n[1] + C'_n[2]$. Thus, after we expand the kth factor in (23) into $2(M+1)(M+2)$ terms for each $k = 1, \dots, m$ and further plug the expansions into "cumulant" C'_n, then using the multilinearity we get a sum of $n \cdot 2(M+1)(M+2)$ "cumulants." For each of those, we apply Theorem 2.10 to reduce them to the conventional cumulants. At this point, most of the terms vanish, as they involve the conventional cumulant of a constant (in fact, zero) random variable. In order $L^{-n/2}$, the only remaining term is $L^{-n/2}$ times the conventional cumulant of $\Delta\mathcal{O}(x_1, y), \dots, \Delta\mathcal{O}(x_n, y)$. Since by [13], Lemma 4.2, the entire sum, C'_n, is $o(L^{-n/2})$, we conclude that the latter cumulant, C_n, is $o(L^{n/2})$. □

2.7. $\mathfrak{q} \to 0$ *limit*. Here we prove Proposition 2.3. Although an extension of this computation to the case of general α is possible, we do not address it here.

At $\alpha = 0$, we take the statement of Theorem 2.1 and absorb 1 as the residue at 0 of the contour integral, getting the formula

$$\mathfrak{q}^{\mathbf{h}(x,y)} = \frac{1}{2\pi\mathbf{i}} \oint \exp\left(\ln(\mathfrak{q})\left(-x\frac{\mathfrak{s}z}{1+\mathfrak{s}z} + y\frac{z}{1+z}\right)\right)\frac{dz}{z}, \tag{24}$$

with integration contour enclosing 0 and -1, but not $-\mathfrak{s}^{-1}$. At this point, we restrict ourselves to the case

$$\mathfrak{s} \le \frac{x}{y} \le \mathfrak{s}^{-1}. \tag{25}$$

The $\mathfrak{q} \to 0$ limit means that $\ln(\mathfrak{q})$ is a large parameter. We study the asymptotics of (24) through the steepest descent method. We thus need to find critical points of the argument of the exponent, that is, to solve

$$0 = \frac{\partial}{\partial z}\left(-x\frac{\mathfrak{s}z}{1+\mathfrak{s}z} + y\frac{z}{1+z}\right) = -\frac{\mathfrak{s}x}{(1+\mathfrak{s}z)^2} + \frac{y}{(1+z)^2}. \tag{26}$$

The solutions z_c are given by

$$\frac{1+\mathfrak{s}z_c}{1+z_c} = \pm\sqrt{\frac{\mathfrak{s}x}{y}}, \qquad z_c = \frac{1-(\pm\sqrt{\frac{\mathfrak{s}x}{y}})}{\pm\sqrt{\frac{\mathfrak{s}x}{y}} - \mathfrak{s}}, \qquad 1+\mathfrak{s}z_c = \frac{\mathfrak{s}^{-1}-1}{\mathfrak{s}^{-1} - (\pm\sqrt{\frac{y}{\mathfrak{s}x}})}. \tag{27}$$

We need the solution with

$$\frac{\partial^2}{\partial z^2}\left(-x\frac{\mathfrak{s}z}{1+\mathfrak{s}z} + y\frac{z}{1+z}\right) < 0,$$

as we want the steepest descent contour to be orthogonal to the real axis (note that our large parameter $\ln(\mathfrak{q})$ is negative). That is, we need

$$2\frac{\mathfrak{s}^2 x}{(1+\mathfrak{s}z)^3} - 2\frac{y}{(1+z)^3} < 0,$$

which is true if

$$\begin{cases} \left(\frac{1+\mathfrak{s}z}{1+z}\right)^3 > \frac{\mathfrak{s}^2 x}{y}, \\ 1+\mathfrak{s}z > 0, \end{cases} \quad \text{or} \quad \begin{cases} \left(\frac{1+\mathfrak{s}z}{1+z}\right)^3 < \frac{\mathfrak{s}^2 x}{y}, \\ 1+\mathfrak{s}z < 0. \end{cases} \tag{28}$$

Note that due to (25) and (27), $1+\mathfrak{s}z_c > 0$ for both solutions Therefore, the solution with $-\sqrt{\frac{\mathfrak{s}x}{y}}$ does not satisfy (28), while the second one does. We conclude that the correct solution has $+\sqrt{\frac{\mathfrak{s}x}{y}}$ in (27), that is,

$$z_c = \frac{1-\sqrt{\frac{\mathfrak{s}x}{y}}}{\sqrt{\frac{\mathfrak{s}x}{y}} - \mathfrak{s}}.$$

Using (25), we see that $z_c > 0$ and, therefore, we can deform the contour in (24) to run through the critical point. The usual critical point approximation arguments show that the integral then behaves as

$$\mathfrak{q}^{\mathbf{h}(x,y)} \sim \exp\left(\ln(\mathfrak{q})\left(-x\frac{\mathfrak{s}z_c}{1+\mathfrak{s}z_c} + y\frac{z_c}{1+z_c}\right)\right)\frac{1}{z_c} \cdot \frac{1}{2\pi\mathbf{i}}\int_{-\mathbf{i}\infty}^{\mathbf{i}\infty} \exp(\kappa_c u^2)\, du, \tag{29}$$

where κ_c is half of the second derivative at the critical point—the integral is evaluated to $\sqrt{2\pi/\kappa_c}$. Therefore,

$$\lim_{\mathfrak{q}\to 0} \mathbf{h}(x,y) = -x\frac{\mathfrak{s}z_c}{1+\mathfrak{s}z_c} + y\frac{z_c}{1+z_c} = \frac{(\sqrt{\mathfrak{s}x}-\sqrt{y})^2}{1-\mathfrak{s}}, \tag{30}$$

which is precisely (8). By combinatorics of the model, $\mathbf{h}(x,y) = 0$ for $x/y = \mathfrak{s}^{-1}$ implies that also $\mathbf{h}(x,y) = 0$ for all $x/y > \mathfrak{s}^{-1}$, as there are no paths to the right from the line $x/y = \mathfrak{s}^{-1}$. Similarly, $\mathbf{h}(x,y) = y - x$ for $x/y = \mathfrak{s}$ implies that $\mathbf{h}(x,y) = y - x$ for $x/y < \mathfrak{s}$, as there is maximal possible number of paths to the left from the line $x/y = \mathfrak{s}$. In the formula (6), this can be also seen: the integral will now be dominated not by the neighborhood of the critical point, but by the residue at 0 or ∞, which appears when we deform the contour to reach the critical point.

3. Four-point relation. All our results for more general (than domain wall) boundary conditions are based on the following statement.

THEOREM 3.1. *Consider the stochastic six-vertex model in the quadrant with arbitrary (possibly, even random) boundary conditions. For each $x, y \geq 0$, we have an identity*

$$\begin{aligned} &q^{H(x+1,y+1)} - b \cdot q^{H(x,y+1)} - bq \cdot q^{H(x+1,y)} + (b + bq - 1) \cdot q^{H(x,y)} \\ &\quad = \xi(x+1, y+1), \end{aligned} \tag{31}$$

where the conditional expectation and variance for ξ are

$$\mathbb{E}\big[\xi(x+1,y+1) \mid H(u,v), u \leq x \text{ or } v \leq y\big] = 0, \tag{32}$$

$$\begin{aligned} &\mathbb{E}\big[\xi^2(x+1,y+1) \mid H(u,v), u \leq x \text{ or } v \leq y\big] \\ &\quad = \big(qb(1-b) + b(1-qb)\big)\Delta_x\Delta_y + b(1-qb)(1-q)q^{H(x,y)}\Delta_x \\ &\qquad - b(1-b)(1-q)q^{H(x,y)}\Delta_y, \end{aligned} \tag{33}$$

with

$$\Delta_x = q^{H(x+1,y)} - q^{H(x,y)}, \qquad \Delta_y = q^{H(x,y+1)} - q^{H(x,y)}.$$

REMARK 3.2. The relation (32) implies that $\xi(x,y)$ are uncorrelated, that is, $\mathbb{E}\xi(x,y)\xi(x',y') = 0$ for any $(x,y) \neq (x',y')$.

PROOF OF THEOREM 3.1. Let us denote $H(x, y)$ through h. We fix the types of vertices at positions (x, y), $(x + 1, y)$, $(x, y + 1)$ and sample the vertex at $(x + 1, y + 1)$ according to the probabilities of Figure 3. There are four cases to consider.

1. If no paths enter into the vertex $(x + 1, y + 1)$ from below or from the left, then the type of the vertex is I and $H(x+1, y) = H(x, y+1) = H(x+1, y+1) = h$, $\Delta_x = \Delta_y = 0$. In particular, $\xi(x + 1, y + 1) = 0$ and, therefore, its conditional expectation and variance vanish, which agrees with (32), (33).

2. If two paths enter into the vertex $(x+1, y+1)$ (one from below and one from the left), then the type of the vertex is II, and $H(x + 1, y) = h - 1$, $H(x, y + 1) = h + 1$, $H(x + 1, y + 1) = h$, $\Delta_x = q^h(q^{-1} - 1)$, $\Delta_y = q^h(q - 1)$. This implies $\xi(x+1, y+1) = q^h(1 - bq - bq \cdot q^{-1} - (1 - b - bq)) = 0$. Again, the conditional expectation and variance vanish matching (32), (33).

3. If the path enters into the vertex $(x + 1, y + 1)$ from below, but no path enters from the left, then we choose between the vertex types IV and VI with probabilities bq and $1 - bq$, respectively. In both cases, $H(x + 1, y) = h - 1$, $H(x, y + 1) = h$, $\Delta_x = q^h(q^{-1} - 1)$, $\Delta_y = 0$. In the first case of type IV, $H(x + 1, y + 1) = h - 1$ and

$$\xi(x + 1, y + 1) = q^h\bigl(q^{-1} - b - bq \cdot q^{-1} + (b + bq - 1)\bigr) = q^h\bigl(q^{-1} - b\bigr)(1 - q).$$

In the second case of type VI, $H(x + 1, y + 1) = h$ and

$$\xi(x + 1, y + 1) = q^h\bigl(1 - b - bq \cdot q^{-1} + (b + bq - 1)\bigr) = q^h b(q - 1).$$

The conditional expectation of $\xi(x + 1, y + 1)$ becomes

$$bq \cdot q^h\bigl(q^{-1} - b\bigr)(1 - q) + (1 - bq) \cdot q^h b(q - 1) = 0.$$

The conditional variance is

$$\begin{aligned} &bq \cdot \bigl(q^h\bigl(q^{-1} - b\bigr)(1 - q)\bigr)^2 + (1 - bq)\bigl(q^h b(q - 1)\bigr)^2 \\ &\quad = b(1 - bq)(1 - q)\bigl(q^{-1} - 1\bigr)q^{2h}, \end{aligned}$$

which matches (33).

4. If the path enters into the vertex $(x+1, y+1)$ from the left, but no path enters from below, then we choose between the vertex types III and V with probabilities b and $1 - b$, respectively. In both cases, $H(x + 1, y) = h$, $H(x, y + 1) = h + 1$, $\Delta_x = 0$, $\Delta_y = q^h(q - 1)$. In the first case of type III, $H(x + 1, y + 1) = h + 1$ and

$$\xi(x + 1, y + 1) = q^h\bigl(q - b \cdot q - bq + (b + bq - 1)\bigr) = q^h(1 - b)(q - 1).$$

In the second case of type V, $H(x + 1, y + 1) = h$ and

$$\xi(x + 1, y + 1) = q^h\bigl(1 - b \cdot q - bq + (b + bq - 1)\bigr) = q^h b(1 - q).$$

The conditional expectation of $\xi(x + 1, y + 1)$ becomes

$$b \cdot q^h(1 - b)(q - 1) + (1 - b) \cdot q^h b(1 - q) = 0.$$

The conditional variance of $\xi(x+1, y+1)$ is

$$b \cdot \big(q^h(1-b)(q-1)\big)^2 + (1-b) \cdot \big(q^h b(1-q)\big)^2 = b(1-b)(1-q)^2 q^{2h},$$

which matches (33). □

At times, it will be convenient to use the integrated form of (31).

COROLLARY 3.3. *In the notation of Theorem 3.1, for each $X, Y \geq 1$, we have*

$$\begin{aligned} & -(1-b)\sum_{x=1}^{X-1} q^{H(x,0)} - (1-bq)\sum_{y=1}^{Y-1} q^{H(0,y)} + (1-b)\sum_{x=1}^{X-1} q^{H(x,Y)} \\ & \quad + (1-bq)\sum_{y=1}^{Y-1} q^{H(X,y)} + (b+bq-1)q^{H(0,0)} - bq \cdot q^{H(X,0)} \\ & \quad - b \cdot q^{H(0,Y)} + q^{H(X,Y)} \\ & = \sum_{x=1}^{X}\sum_{y=1}^{Y} \xi(x,y). \end{aligned} \tag{34}$$

PROOF. We sum (31) over $x = 0, \ldots, X-1$, $y = 0, \ldots, Y-1$. □

4. The telegraph partial differential equation. We saw in Theorem 2.1 and equation (9) that the limit shape (after a nonlinear transformation) solves the telegraph equation. In order to move forward, we need to collect the facts about this equation and its solutions. Some parts of this section are based on [28], Chapter V.

4.1. *Existence and uniqueness of solutions*. Take three arbitrary real parameters λ, μ, ν and a continuous function $g(x, y) : \mathbb{R}_{\geq 0} \times \mathbb{R}_{\geq 0} \to \mathbb{R}$. Consider the following integral equation for an unknown continuous function $\phi(x, y)$, $x \geq 0$, $y \geq 0$:

$$\begin{aligned} & \phi(X,Y) + \lambda \int_0^X \phi(x,Y)\,dx + \mu \int_0^Y \phi(X,y)\,dy \\ & \quad + \nu \int_0^X \int_0^Y \phi(x,y)\,dx\,dy = g(X,Y). \end{aligned} \tag{35}$$

PROPOSITION 4.1. *For each $a, b > 0$, the equation (35) has a continuous solution $\phi(x, y)$ in $[0, a] \times [0, b]$. The solution is unique.*

PROOF. Because of the invariance of the form of the equation with respect to translations, it suffices to prove the claim for small a and b; we will require that

$$\big(|\lambda| + |\mu| + |\nu|\big)(a + b + ab) < 1.$$

Let $\mathbf{C}_{a,b}$ denote the Banach space of continuous functions on $[0,a]\times[0,b]$ equipped with the supremum norm. Let $\Theta:\mathbf{C}_{a,b}\to\mathbf{C}_{a,b}$ be defined through

$$[\Theta f](X,Y) = g(X,Y) - \lambda\int_0^X f(x,Y)\,dx - \mu\int_0^Y f(X,y)\,dy - \nu\int_0^X\int_0^Y f(x,y)\,dx\,dy.$$

We claim that for sufficiently small a, b the map Θ is a contraction. Indeed,

$$\begin{aligned}\|\Theta f_1 - \Theta f_2\| &= \sup_{0\le X\le a, 0\le Y\le b}\bigg|\lambda\int_0^X \big(f_1(x,Y)-f_2(x,Y)\big)\,dx \\ &\quad + \mu\int_0^Y \big(f_1(X,y)-f_2(X,y)\big)\,dy + \nu\int_0^X\int_0^Y \big(f_1(x,y)-f_2(x,y)\big)\,dx\,dy\bigg| \\ &\le \big(|\lambda|+|\mu|+|\nu|\big)(a+b+ab)\|f_1-f_2\|.\end{aligned}$$

By the contraction mapping principle (Banach fixed-point theorem), there exists a unique ϕ such that $\Theta\phi=\phi$, which gives the unique solution to (35). $\square$

Differentiating (35), we rewrite it as a partial differential equation (with $\tilde g = g_{xy}$)

$$\phi_{xy}(x,y) + \lambda\phi_y(x,y) + \mu\phi_x(x,y) + \nu\phi(x,y) = \tilde g(x,y), \quad x,y>0. \tag{36}$$

For various choices of λ, μ, ν and $\tilde g$ this equation has various names, for example, the telegraph equation or Klein–Gordon equation.

The solutions to (36) with different λ, μ, ν are readily related to each other by an observation that if ϕ solves (36), then $\psi(x,y)=e^{wx+vy}\phi(x,y)$ solves

$$\begin{aligned}&\psi_{xy} + (\lambda-w)\psi_y + (\mu-v)\psi_x + (\nu - w\mu - v\lambda + wv)\psi \\ &\quad = \tilde g(x,y)\exp(wx+vy).\end{aligned} \tag{37}$$

PROPOSITION 4.2. *Take $a,b>0$ and consider the equation (36) on an unknown continuous function $\phi:[0,a]\times[0,b]\to\mathbb{R}$ with continuous mixed derivative ϕ_{xy} in the interior of the rectangle. If $\tilde g(x,y)$ is continuous, and (36) is supplemented with boundary condition*

$$\phi(x,0)=\chi(x), \qquad \phi(0,y)=\psi(y),$$

with given continuously differentiable χ and ψ that have the same value at the origin, then (36) has a unique solution.

REMARK 4.3. When the boundary data or $\tilde g(x,y)$ are less regular, then one need to understand the solution ϕ in a generalized sense through (35), (38). In the next section, we provide an explicit formula (42) for the solution, which can be also used for extending to more general initial data; see Remark 4.5 below.

PROOF OF PROPOSITION 4.2. Using transformation (37) if necessary, we may and will consider only the case $\lambda = \mu = 0$. We integrate the equation to get

$$\phi(X,Y) - \phi(X,0) - \phi(0,Y) + \phi(0,0) + \nu \int_0^X \int_0^Y \phi(x,y)\,dx\,dy = \int_0^X \int_0^Y \tilde{g}(x,y)\,dx\,dy, \tag{38}$$

which is (35) with

$$g(X,Y) = \int_0^X \int_0^Y \tilde{g}(x,y)\,dx\,dy + \chi(X) + \psi(Y) - \chi(0).$$

By Proposition 4.1, there is a unique continuous solution. Since $\phi(X,Y)$ in (38) is given by the sum of double integrals of continuous functions and two other continuously differentiable functions, its mixed partial derivative exists and is continuous. Thus, we can differentiate (38) returning to (36). □

4.2. *Solutions as contour integral.* Define the *Riemann function* (for the equation (40) below) through

$$\mathcal{R}(X,Y;x,y) = \frac{1}{2\pi \mathbf{i}} \oint_{-\beta_1} \frac{(\beta_2 - \beta_1)\,dz}{(z+\beta_1)(z+\beta_2)} \times \exp\left[(\beta_1 - \beta_2)\left(-(X-x)\frac{z}{z+\beta_2} + (Y-y)\frac{z}{z+\beta_1}\right)\right], \tag{39}$$

where the integration goes in positive direction and encircles $-\beta_1$, but not $-\beta_2$. Note that we can also integrate in the negative direction around $-\beta_2$ for the same result, because the residue of the integrand at infinity vanishes.

THEOREM 4.4. *Consider the equation*

$$\phi_{XY}(X,Y) + \beta_1 \phi_Y(X,Y) + \beta_2 \phi_X(X,Y) = u(X,Y), \quad X, Y > 0, \tag{40}$$

with boundary conditions

$$\phi(x,0) = \chi(x), \qquad \phi(0,y) = \psi(y), \tag{41}$$

where χ and ψ are continuously differentiable with $\psi(0) = \chi(0)$. The solution (*afforded by Proposition* 4.2) *has the form*

$$\begin{aligned}\phi(X,Y) &= \psi(0)\mathcal{R}(X,Y;0,0) \\ &\quad + \int_0^Y \mathcal{R}(X,Y;0,y)\big(\psi'(y) + \beta_2 \psi(y)\big)\,dy \\ &\quad + \int_0^X \mathcal{R}(X,Y;x,0)\big(\chi'(x) + \beta_1 \chi(x)\big)\,dx \\ &\quad + \int_0^X \int_0^Y \mathcal{R}(X,Y;x,y) u(x,y)\,dx\,dy.\end{aligned} \tag{42}$$

REMARK 4.5. If we integrate by parts the terms involving $\psi'(y)$ and $\chi'(x)$ in (42), then using the smoothness $\mathcal{R}(X, Y; x, y)$ we get an expression which continuously depends on the boundary data $\psi(y)$, $\chi(x)$ (in the supremum norm). This can be used to define the solution to (40) for nondifferentiable $\chi(x)$, $\psi(y)$.

PROOF OF THEOREM 4.4. The function $\mathcal{R}(X, Y; x, y)$ satisfies the following properties, which are checked by direct differentiation under the integral sign:

1. $\mathcal{R}_{XY} + \beta_1 \mathcal{R}_Y + \beta_2 \mathcal{R}_X = 0$,
2. $[\mathcal{R}_X + \beta_1 \mathcal{R}]_{Y=y} = 0 = [\mathcal{R}_x - \beta_1 \mathcal{R}]_{Y=y}$,
3. $[\mathcal{R}_Y + \beta_2 \mathcal{R}]_{X=x} = 0 = [\mathcal{R}_y - \beta_2 \mathcal{R}]_{X=x}$,
4. $[\mathcal{R}]_{X=x, Y=y} = 1$.

Using these properties, we apply the differential operator $F \mapsto F_{XY} + \beta_1 F_Y + \beta_2 F_X$ to each term in (42). The first term gives 0 by the first property. The second term gives (using the first two properties)

$$\begin{aligned}&\int_0^Y \big(\mathcal{R}_{XY}(X, Y; 0, y) + \beta_1 \mathcal{R}_Y(X, Y; 0, y) + \beta_2 \mathcal{R}_X(X, Y; 0, y)\big)\\ &\qquad \times \big(\psi'(y) + \beta_2 \psi(y)\big)\, dy\\ &\qquad + \big[\big(\mathcal{R}_X(X, Y; 0, y) + \beta_1 \mathcal{R}(X, Y, 0, y)\big)\big(\psi'(y) + \beta_2 \psi(y)\big)\big]_{y=Y}\\ &\quad = 0.\end{aligned}$$

The third term also vanishes by similar reasoning with the first and third properties. The fourth term gives (using all four properties)

$$\begin{aligned}&\int_0^X \int_0^Y \big(\mathcal{R}_{XY}(X, Y; x, y) + \beta_1 \mathcal{R}_Y(X, Y; x, y)\\ &\qquad + \beta_2 \mathcal{R}_X(X, Y; x, y)\big) u(x, y)\, dx\, dy\\ &\qquad + \int_0^X \big[\mathcal{R}_X(X, Y; x, y) + \beta_1 \mathcal{R}(X, Y; x, y)\big]_{y=Y}\, dx\\ &\qquad + \int_0^Y \big[\mathcal{R}_Y(X, Y; x, y) + \beta_2 \mathcal{R}(X, Y; x, y)\big]_{x=X}\, dy\\ &\qquad + \big[\mathcal{R}(X, Y; x, y) u(x, y)\big]_{x=X, y=Y}\\ &\quad = u(X, Y).\end{aligned}$$

We conclude that (42) satisfies (40). It remains to check the boundary conditions. At $X = 0$, the third and fourth terms in (42) vanish. Integrating by parts and using the third and fourth properties, we obtain

$$\psi(0) \cdot \mathcal{R}(0, Y; 0, 0) + \int_0^Y \mathcal{R}(0, Y; 0, y)\big(\psi'(y) + \beta_2 \psi(y)\big)\, dy$$

$$= \mathcal{R}(0, Y; 0, Y)\psi(Y) - \int_0^Y \big(\mathcal{R}_y(0, Y; 0, y) - \beta_2\mathcal{R}(0, Y; 0, y)\big)\psi(y)\,dy$$
$$= \psi(Y).$$

At $Y = 0$, the second and fourth terms in (42) vanish. Integrating by parts and using the second and fourth properties, we then get

$$\chi(0)\mathcal{R}(X, 0; 0, 0) + \int_0^X \mathcal{R}(X, 0; x, 0)\big(\chi'(x) + \beta_1\chi(x)\big)\,dx$$
$$= \chi(X)\mathcal{R}(X, 0; X, 0)$$
$$+ \int_0^X \big(\mathcal{R}_x(X, 0; x, 0) - \beta_1\mathcal{R}(X, 0, x, 0)\big)\chi(x)\,dx = \chi(X). \qquad \square$$

4.3. *Discretization.* The telegraph equation has a natural discretization, which we present here. (We have not seen it in the literature before.)

Consider the following equation for an unknown function $\Phi(x, y)$, $x, y = 0, 1, 2, \dots$:

$$\begin{aligned}\Phi(x+1, y+1) - b_1\Phi(x, y+1) - b_2\Phi(x+1, y)&\\ + (b_1 + b_2 - 1)\Phi(x, y)&\\ = u(x+1, y+1)&\end{aligned} \tag{43}$$

with a given right-hand side u and subject to boundary conditions

$$\Phi(x, 0) = \chi(x), \qquad \Phi(0, y) = \psi(Y), \quad X, Y = 0, 1, 2, \dots, \chi(0) = \psi(0). \tag{44}$$

We take b_1 and b_2 to be arbitrary distinct real numbers satisfying $0 < b_1, b_2 < 1$. Although, these restrictions can be easily removed if needed (this mould lead to natural modifications of the formulas below).

PROPOSITION 4.6. *The equations* (43), (44) *have a unique solution.*

PROOF. Using (43) and starting from (44), we recursively define the values of $\Phi(x, y)$ first for the point $(1, 1)$, then for the points $(1, 2)$, $(2, 1)$, then for the points $(1, 3)$, $(2, 2)$, $(3, 1)$, etc. $\square$

Define the discrete Riemann function through

$$\begin{aligned}&\mathcal{R}^d(X, Y; x, y)\\ &\quad = \frac{1}{2\pi\mathbf{i}}\oint_{-\frac{1}{b_2(1-b_1)}} \frac{(b_2 - b_1)\,dz}{(1 + b_2(1-b_1)z)(1 + b_1(1-b_2)z)}\\ &\qquad \times \left(\frac{1 + b_1(1-b_1)z}{1 + b_2(1-b_1)z}\right)^{X-x}\left(\frac{1 + b_2(1-b_2)z}{1 + b_1(1-b_2)z}\right)^{Y-y},\end{aligned} \tag{45}$$

where the integration goes in positive direction and encircles $-\frac{1}{b_2(1-b_1)}$, but not $-\frac{1}{b_1(1-b_2)}$. Note that we can also integrate in the negative direction around $-\frac{1}{b_1(1-b_2)}$ for the same result.

THEOREM 4.7. *The solution to* (43), (44) *has the form*

$$\begin{aligned}\Phi(X,Y) = {}& \chi(0)\mathcal{R}^d(X,Y;0,0)\\ &+ \sum_{y=1}^{Y} \mathcal{R}^d(X,Y;0,y)\big(\psi(y) - b_2\psi(y-1)\big)\\ &+ \sum_{x=1}^{X} \mathcal{R}^d(X,Y;x,0)\big(\chi(x) - b_1\chi(x-1)\big)\\ &+ \sum_{x=1}^{X}\sum_{y=1}^{Y} \mathcal{R}^d(X,Y;x,y)u(x,y).\end{aligned} \tag{46}$$

PROOF. Directly from the definition, we see that the function $\mathcal{R}^d$ satisfies:

1. $\mathcal{R}^d(X+1,Y+1) - b_1\mathcal{R}^d(X,Y+1) - b_2\mathcal{R}^d(X+1,Y) + (b_1+b_2-1)\mathcal{R}^d(X,Y) = 0$,
2. $[\mathcal{R}^d(X+1) - b_1\mathcal{R}^d(X)]_{y=Y} = 0 = [\mathcal{R}^d(x-1) - b_1\mathcal{R}^d(x)]_{y=Y}$,
3. $[\mathcal{R}^d(Y+1) - b_2\mathcal{R}^d(Y)]_{x=X} = 0 = [\mathcal{R}^d(y-1) - b_2\mathcal{R}^d(y)]_{x=X}$,
4. $[\mathcal{R}^d(X,Y;x,y)]_{x=X,y=Y} = 1$.

We apply the difference operator $F \mapsto F(X+1,Y+1) - b_1F(X,Y+1) - b_2F(X+1,Y) + (b_1+b_2-1)F(X,Y)$ to each of the four terms of (46) using the properties of $\mathcal{R}^d$. The first term gives zero by the first property. The second term gives (using the first and second properties)

$$\begin{aligned}&\sum_{y=1}^{Y}\big(\mathcal{R}^d(X+1,Y+1;0,y) - b_1\mathcal{R}^d(X,Y+1;0,y)\\ &\quad - b_2\mathcal{R}^d(X+1,Y;0,y)\\ &\quad + (b_1+b_2-1)\mathcal{R}^d(X,Y;0,y)\big)\big(\psi(y) - b_2\psi(y-1)\big)\\ &\quad + \big(\mathcal{R}^d(X+1,Y+1;0,Y+1) - b_1\mathcal{R}^d(X,Y+1;0,Y+1)\big)\\ &\quad \times \big(\psi(Y+1) - b_2\psi(Y)\big) = 0.\end{aligned} \tag{47}$$

The third term gives zero for similar reasons via the first and third properties. The fourth term gives (using all four properties)

$$\sum_{x=1}^{X}\sum_{y=1}^{Y}\big(\mathcal{R}^d(X+1,Y+1;x,y) - b_1\mathcal{R}^d(X,Y+1;x,y)$$

$$
\begin{aligned}
&- b_2\mathcal{R}^d(X+1, Y; x, y) \\
&+ (b_1+b_2-1)\mathcal{R}^d(X, Y; x, y)\big)u(x, y) \\
&+ \sum_{x=1}^{X}\big(\mathcal{R}^d(X+1, Y+1; x, Y+1) \\
&- b_1\mathcal{R}^d(X, Y+1; x, Y+1)\big)u(x, Y+1) \qquad (48)\\
&+ \sum_{y=1}^{Y}\big(\mathcal{R}^d(X+1, Y+1; X+1, y) \\
&- b_2\mathcal{R}^d(X+1, Y; X+1, y)\big)u(X+1, y) \\
&+ \mathcal{R}^d(X+1, Y+1; X+1, Y+1)u(X+1, Y+1) \\
= {}& u(X+1, Y+1).
\end{aligned}
$$

We conclude that (46) satisfies (43), and it remains to check the boundary conditions.

At $X = 0$, note that by the third property of $\mathcal{R}^d$, $\mathcal{R}^d(0, Y; 0, y) = b_2^{-y}\mathcal{R}^d(0, Y; 0, 0)$. Therefore, we have (using the fourth property as well)

$$
\begin{aligned}
\Phi(0, Y) &= \mathcal{R}^d(0, Y; 0, 0)\left(\psi(0) + \sum_{y=1}^{Y} b_2^{-y}\big(\psi(y) - b_2\psi(y-1)\big)\right) \\
&= \mathcal{R}^d(0, Y; 0, 0)\psi(Y)b_2^{-Y} = \mathcal{R}^d(0, Y; 0, Y)\psi(Y) = \psi(Y).
\end{aligned} \tag{49}
$$

At $Y = 0$, by the second property, $\mathcal{R}^d(X, 0; x, 0) = b_1^{-x}\mathcal{R}^d(X, 0; 0, 0)$, and thus,

$$
\begin{aligned}
\Phi(X, 0) &= \mathcal{R}^d(X, 0; 0, 0)\left(\chi(0) + \sum_{x=1}^{X} b_1^{-x}\big(\chi(x) - b_1\chi(x-1)\big)\right) \\
&= \mathcal{R}^d(X, 0; 0, 0)\chi(X)b_1^{-X} = \mathcal{R}^d(X, 0; X, 0)\chi(X) = \chi(X).
\end{aligned} \tag{50}
$$

□

4.4. *Solutions as path integrals*: *Discrete case*. In this section, we interpret the formula of Theorem 4.7 as an expectation of a certain path integral. Essentially, this is a development of a version of the Feynman–Kac formula for the difference equation (43).

Consider a random path that starts at a point (X, Y) in the positive quadrant and moves in the direction of decreasing x and y. At each step, the path moves by one to the left, or down, or makes a turn. The choices are made according to probabilities of Figure 4. These weights are obtained from the weights of Figure 3 by central symmetry $(x, y) \mapsto (-x, -y)$. In other words, the weights of the straight segments remained the same, while the weights of corners were swapped in order to preserve stochasticity.

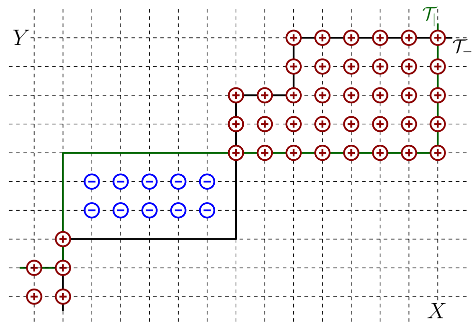

FIG. 5. *Two paths $\mathcal{T}_-$, $\mathcal{T}_|$ and the function $\mathcal{I}_{\text{between}}(x, y)$: values $+1$ and -1 are shown by $\oplus$ and $\ominus$, respectively.*

THEOREM 4.8. *Consider the equation* (43), (44) *with* $u(X, Y) = 0$, $X, Y \geq 0$, *and* $\chi(0) = \psi(0) = 0$. *For convenience, extend* $\chi(-a) = \psi(-a) = 0$, $a > 0$. *The solution* $\Phi(X, Y)$ *admits the following stochastic formula. Take a* (*reversed, with probabilities of Figure* 4) *path leaving* $(X + 1, Y)$ *to the left in horizontal direction, and let* $\mathbf{y}$ *denote the ordinate of the first point when it reaches the line* $x = 0$. *Take another path leaving* $(X, Y + 1)$ *down in vertical direction, and let* $\mathbf{x}$ *denote the abscissa of the first point when it reaches the line* $y = 0$. *Then*

$$\Phi(X, Y) = \mathbb{E}[\psi(\mathbf{y})] + \mathbb{E}[\chi(\mathbf{x})]. \tag{51}$$

We will give a proof a little later, and now we will see what happens when $u \neq 0$.

Suppose that we are given a trajectory $\mathcal{T}$ of a path build out of the blocks of Figure 4. For a point $(x, y) \in \mathbb{Z} \times \mathbb{Z}$, we say that (x, y) is *weakly below* $\mathcal{T}$, if any of the points of the square $(x - 1/2, x + 1/2) \times (y - 1/2, y + 1/2)$ is below (i.e., has a smaller vertical coordinate and the same horizontal coordinate) than a point of the path. Similarly, we say that (x, y) is *weakly to the left* from $\mathcal{T}$, if any point of $(x - 1/2, x + 1/2) \times (y - 1/2, y + 1/2)$ is to the left of a point of the path.

Now suppose that we are given two paths $\mathcal{T}_-$ and $\mathcal{T}_|$. Define

$$\begin{aligned}\mathcal{I}_{\text{between}}(x, y) = \mathbf{1}&_{(x,y) \text{ is weakly below } \mathcal{T}_-} \\ &+ \mathbf{1}_{(x,y) \text{ is weakly to the left from } \mathcal{T}_|} - 1.\end{aligned} \tag{52}$$

In other words, $\mathcal{I}_{\text{between}}(x, y)$ is ± 1 between the paths $\mathcal{T}_-$, $\mathcal{T}_+$ and vanishes otherwise. The sign depends on which path is higher. An illustration of the values of this function is shown in Figure 5.

THEOREM 4.9. *Consider the equation* (43), (44) *with* $\chi(x) = \psi(y) = 0$, $x, y \geq 0$. *The solution* $\Phi(X, Y)$ *admits the following stochastic formula. Take a* (*reversed, with probabilities of Figure* 4) *path* $\mathcal{T}_-$ *leaving* $(X + 1, Y)$ *to the left* *in horizontal direction and another path* $\mathcal{T}_|$ *leaving* $(X, Y+1)$ *down in vertical direction. Then*

$$\Phi(X,Y) = \mathbb{E}\left[\sum_{x=1}^{X}\sum_{y=1}^{Y} u(x,y)\mathcal{I}_{\text{between}}(x,y)\right], \tag{53}$$

where we use the definition (52). *In words*, $\Phi(X,Y)$ *is the expected signed sum of all the inhomogeneities of* (43) *between the paths*.

By linearity of the equation, the solution to (43) when both u and χ, ψ are nonvanishing is the sum of the right-hand sides in (51), (53).

COROLLARY 4.10. *In the notation of Theorem* 4.8, 4.9 *consider the case when both* $u(x,y)$ *and* χ, ψ *are nonvanishing. Then*

$$\Phi(X,Y) = \mathbb{E}\big[\psi(\mathbf{y})\big] + \mathbb{E}\big[\chi(\mathbf{x})\big] + \mathbb{E}\left[\sum_{x=1}^{X}\sum_{y=1}^{Y} u(x,y)\mathcal{I}_{\text{between}}(x,y)\right]. \tag{54}$$

PROOF OF THEOREM 4.8. By linearity, it suffices to consider the case

$$\chi \equiv 0, \qquad \psi(y) = \begin{cases} 1 & y = y_0, \\ 0 & \text{otherwise}. \end{cases} \tag{55}$$

In this case, the right-hand side of (51) becomes the probability of intersecting the line $x = 1/2$ at point $(1/2, y_0)$. Let us compute this probability.

We start by considering a particular case of the stochastic six-vertex model (with the weights of Figure 3 at $\alpha = 0$) when we have only one path. In this case, the expectation of the height function has a simple probabilistic meaning:

$$\begin{aligned} &\mathbb{E}\left[\frac{1 - q^{H(x+1,y)}}{1-q}\right] \\ &\quad = \operatorname{Prob}\big(\text{the path passes to the right from } (x+1/2, y+1/2)\big) \\ &\quad = \operatorname{Prob}\big(\text{the path passes below } (x+1/2, y+1/2)\big). \end{aligned} \tag{56}$$

In this formula, we think about the paths as having integer coordinates, and we introduced shifts by $1/2$ to avoid ambiguity for the case when the path passes exactly through the point of interest.

Suppose that the path enters the positive quadrant through the point $(1, y_0)$ coming from the left. Then by Theorem 3.1, (56) denoted as $F^-_{y_0}(X,Y)$ (the superscript $^-$ indicates that the path enters horizontally) solves

$$\begin{aligned} &F^-_{y_0}(X+1,Y+1) - b_1 F^-_{y_0}(X,Y+1) - b_2 F^-_{y_0}(X+1,Y) \\ &\quad + (b_1+b_2-1)F^-_{y_0}(X,Y) = 0, \end{aligned} \tag{57}$$

with

$$F^-_{y_0}(X,0)=0, \qquad F^-_{y_0}(0,Y)=\begin{cases}0, & Y<y_0,\\ 1, & Y\geq y_0.\end{cases} \tag{58}$$

Theorem 4.7 gives a closed formula:

$$F^-_{y_0}(X,Y)=\mathcal{R}^d(X,Y;0,y_0)+(1-b_2)\sum_{y=y_0+1}^{Y}\mathcal{R}^d(X,Y;0,y). \tag{59}$$

Consider the difference

$$P_{-,-}(0,y_0;X,Y):=F^-_{y_0}(X,Y)-F^-_{y_0}(X,Y-1).$$

Relation (56) implies that it computes the probability that the path, which entered the quadrant horizontally at $(1,y_0)$, ends horizontally at $(X+1/2,Y)$ (i.e., the path *enters into* $(X+1,Y)$ from the left). Using (59), we get

$$\begin{aligned}P_{-,-}(0,y_0;X,Y)=(1-b_2)\sum_{y=y_0+1}^{Y-1}\bigl(&\mathcal{R}^d(X,Y;0,y)\\ &-\mathcal{R}^d(X,Y-1;0,y)\bigr)\\ &+(1-b_2)\mathcal{R}^d(X,Y;0,Y)+\mathcal{R}^d(X,Y;0,y_0)\\ &-\mathcal{R}^d(X,Y-1;0,y_0).\end{aligned} \tag{60}$$

Since $\mathcal{R}^d(X,Y;x,y)$ depends only on differences $X-x$, $Y-y$, the sum telescopes and (60) simplifies to

$$P_{-,-}(0,y_0;X,Y)=\mathcal{R}^d(X,Y;0,y_0)-b_2\mathcal{R}^d(X,Y;0,y_0+1). \tag{61}$$

By translation invariance, the same formula holds for the path which starts not by entering from the left into $(1,y_0)$, but into an arbitrary point (x_0+1,y_0):

$$P_{-,-}(x_0,y_0;X,Y)=\mathcal{R}^d(X,Y;x_0,y_0)-b_2\mathcal{R}^d(X,Y;x_0,y_0+1). \tag{62}$$

Note that this holds for $Y=y_0$ as well, if we agree that $\mathcal{R}^d(X,y_0;x_0,y_0+1)=0$.

By symmetry, we can also obtain similar formulas for the case when the path starts by entering from below into a point (x_0,y_0+1). The probability of this path entering into $(X,Y+1)$ from below is

$$P_{|,|}(x_0,y_0;X,Y)=\mathcal{R}^d(X,Y;x_0,y_0)-b_1\mathcal{R}^d(X,Y;x_0+1,y_0). \tag{63}$$

Let us return to proving (51) in the particular case (55). We need to show that

$$\Phi(X,Y)=P_{-,-}(-X,-Y;0,-y_0). \tag{64}$$

Note that we changed the signs of the coordinates to reflect the fact that the walk in the direction of growing (x,y) with weights of Figure 3 differs from the one from Figure 4 that we need to use.

The definition of $P_{-,-}$ readily implies that (64) satisfies the boundary condition (44), (55). On the other hand, note that since $\mathcal{R}^d(X, Y; x, y)$ depends only on $(X - x)$, $(Y - y)$, the first property in the proof of Theorem 4.7 is equivalent to

$$\begin{aligned} &\mathcal{R}^d(X, Y; x-1, y-1) - b_1\mathcal{R}^d(X, Y; x, y-1) \\ &\quad - b_2\mathcal{R}^d(X, Y; x-1, y) \\ &\quad + (b_1 + b_2 - 1)\mathcal{R}^d(X, Y; x, y) = 0. \end{aligned} \tag{65}$$

Combining (61) with (65), we conclude that (64) satisfies (43). □

PROOF OF THEOREM 4.9. By linearity, it suffices to prove (53) for the case when $u(x, y)$ is nonzero only at one point, where it equals 1. In this case, by Theorem 4.7 the solution is

$$\Phi(X, Y) = \mathbf{1}_{X\geq x_0}\mathbf{1}_{Y\geq y_0}\mathcal{R}^d(X, Y; x_0, y_0).$$

When either $X < x_0$ or $Y < y_0$, matching with (53) is immediate, so we will only consider the case $X \geq x_0$, $Y \geq y_0$. Then (53) suggests that we need to compute the expectation of $\mathcal{I}_{\text{between}}(x_0, y_0)$.

Using the notation from the proof of Theorem 4.8 and (62), (63), we have

$$\begin{aligned} &\mathbb{E}\big[\mathcal{I}_{\text{between}}(x_0, y_0) + 1\big] \\ &\quad = \sum_{y=y_0}^{Y} P_{-,-}(-X, -Y; -x, -y) + \sum_{x=x_0}^{X} P_{|,|}(-X, -Y; -x, -y) \\ &\quad = \sum_{y=y_0}^{Y} \big(\mathcal{R}^d(-x_0, -y; -X, -Y) - b_2\mathcal{R}^d(-x_0, -y; -X, -Y+1)\big) \\ &\qquad + \sum_{x=x_0}^{X} \big(\mathcal{R}^d(-x, -y_0; -X, -Y) - b_1\mathcal{R}^d(-x, -y_0; -X+1, -Y)\big) \\ &\quad = \sum_{y=y_0}^{Y} \big(\mathcal{R}^d(X, Y; x_0, y) - b_2\mathcal{R}^d(X, Y; x_0, y+1)\big) \\ &\qquad + \sum_{x=x_0}^{X} \big(\mathcal{R}^d(X, Y; x, y_0) - b_1\mathcal{R}^d(X, Y; x+1, y_0)\big), \end{aligned} \tag{66}$$

where we agree that $\mathcal{R}^d(X, Y; X+1, y_0) = \mathcal{R}^d(X, Y; x_0, Y+1) = 0$.

On the other hand, let us sum (65) over $x = x_0 + 1, \dots, X + 1$, $y = y_0 + 1, \dots, Y + 1$ except for $(x, y) = (X + 1, Y + 1)$. Note that the formula (45) for $\mathcal{R}^d$ makes sense even when $x > X$ and, moreover, it vanishes identically. This implies that (65) still holds for such x (as its proof is just a computation showing identical vanishing of the integrand). Similarly, we can deform the contour in (45), so that it encloses $-\frac{1}{b_1(1-b_2)}$ instead of $-\frac{1}{b_2(1-b_1)}$. Then the result vanishes for $y > Y$ and, therefore, (65) holds again. Note, however, that we cannot take both $x > X$ and $y > Y$ simultaneously, as then the argument no longer works.

We get

$$\begin{aligned}&\mathcal{R}^d(X,Y;x_0,y_0) + (1-b_1)\sum_{x=x_0+1}^{X}\mathcal{R}^d(X,Y;x,y_0)\\ &\quad + (1-b_2)\sum_{y=y_0+1}^{Y}\mathcal{R}^d(X,Y;x_0,y)\\ &\quad - \mathcal{R}^d(X,Y;X,Y) = 0.\end{aligned} \tag{67}$$

Recall that $\mathcal{R}^d(X,Y;X,Y) = 1$. Thus, (66) turns into

$$\mathbb{E}[\mathcal{I}_{\text{between}}(x_0,y_0)+1] = 1 + \mathcal{R}^d(X,Y;x_0,y_0). \qquad \square$$

4.5. *Solutions as path integrals*: *Continuous case*. In this section, we develop a continuous analogue of Section 4.4 and present the Feynman–Kac formula for the solution of the telegraph equation (40).

The basic stochastic object is the *persistent Poisson random walk*. It starts from $(X,Y) \in \mathbb{R}^2_{>0}$ and moves toward the origin along vertical and horizontal directions. Whenever it moves horizontally, it turns down with intensity $\beta_1 > 0$. Whenever it moves vertically, it turns to the left with intensity $\beta_2 > 0$. This process is the limit of the random walks of Section 4.4 with weights of Figure 4 in the limit regime (4). There is one choice to be made—when the path leaves (X,Y) it can start by going horizontally or vertically. We denote the resulting (random) trajectories through $\mathcal{T}_-$ and $\mathcal{T}_|$, respectively.

THEOREM 4.11. *Consider the telegraph equation* (40), (41). *Assume that* $\psi(0) = \chi(0) = 0$ *and extend these functions to negative arguments as identical zeros*. *The solution* $\phi(X,Y)$ *admits the following stochastic formula*. *Consider two* (*independent*) *persistent Poisson paths* $\mathcal{T}_-$ *and* $\mathcal{T}_|$, *leaving* (X,Y) *horizontally and vertically*, *respectively*. *Let* $\mathbf{y}$ *be the ordinate of the first intersection of* $\mathcal{T}_-$ *with the* y-*axis*, *and let* $\mathbf{x}$ *be the abscissa of the first intersection of* $\mathcal{T}_|$ *with the* x-*axis*. *Further, for any point* $(x,y) \in \mathbb{R}^2_{>0}$, *define*

$$\mathcal{I}_{\text{between}}(x,y) = \begin{cases} 1 & (x,y) \textit{ is between } \mathcal{T}_- \textit{ and } \mathcal{T}_| \textit{ with } \mathcal{T}_- \textit{ above},\\ -1 & (x,y) \textit{ is between } \mathcal{T}_- \textit{ and } \mathcal{T}_| \textit{ with } \mathcal{T}_- \textit{ below},\\ 0 & \textit{otherwise}.\end{cases}$$

Then

$$\phi(X,Y) = \mathbb{E}\chi(\mathbf{x}) + \mathbb{E}\psi(\mathbf{y}) + \mathbb{E}\left[\int_0^X\int_0^Y \mathcal{I}_{\text{between}}(x,y)u(x,y)\,dx\,dy\right]. \tag{68}$$

PROOF. Consider the limit transition (4) with simultaneous rescaling by L of the coordinates x and y, boundary conditions χ, ψ, the right-hand side $u(x, y)$, and the solutions $\Phi(X, Y)$. Then Corollary 4.10 and the straightforward limit relation

$$\lim_{L\to\infty} \mathcal{R}^d(LX, LY; Lx, Ly) = \mathcal{R}(X, Y; x, y),$$

implies that the solution to the difference relation (43) turns into the solution to the telegraph equation (40). Simultaneously, the same limit transition turns the random walks of Section 4.4 into persistent Poisson random walks.

We conclude that (68) is the $L \to \infty$ limit of (54). □

5. Law of large numbers through four-point relation. From now on, we set $\alpha = 0$ and study only the stochastic six-vertex model. Our aim is to extend Theorem 2.1 to arbitrary boundary conditions. Our main technical tool is the four-point relation of Section 3.

5.1. *LLN for general boundary conditions.*

THEOREM 5.1. *Fix $a, b > 0$, take two 1-Lipschitz monotone functions $\chi : [0, a] \to \mathbb{R}$, $\psi : [0, b] \to \mathbb{R}$ such that $\chi(0) = \psi(0)$. Suppose that the boundary condition in the stochastic six-vertex model is chosen so that as $L \to \infty$, $\frac{1}{L}H(Lx, 0) \to \chi(x)$ and $\frac{1}{L}H(0, Ly) \to \psi(y)$ uniformly on $x \in [0, a]$, $y \in [0, b]$.*

Define the function $\mathfrak{q}^{\mathbf{h}} : [0, a] \times [0, b] \to \mathbb{R}$ as the solution to the PDE

$$\frac{\partial^2}{\partial x\, \partial y}\left(\mathfrak{q}^{\mathbf{h}(x,y)}\right) + \beta_2 \frac{\partial}{\partial x}\left(\mathfrak{q}^{\mathbf{h}(x,y)}\right) + \beta_1 \frac{\partial}{\partial y}\left(\mathfrak{q}^{\mathbf{h}(x,y)}\right) = 0,$$
$$\mathfrak{q}^{\mathbf{h}(x)} = \chi(x), \qquad \mathfrak{q}^{\mathbf{h}(0,y)} = \psi(y, 0). \tag{69}$$

Then the height function of the stochastic six-vertex model ($\alpha = 0$) *satisfies the law of large numbers in the limit regime* (4):

$$\lim_{L\to\infty} \sup_{(x,y)\in[0,a]\times[0,b]} \left| \frac{1}{L} H(Lx, Ly) - \mathbf{h}(x, y) \right| = 0 \quad \textit{in probability.} \tag{70}$$

REMARK 5.2. Proposition 4.2 says that (69) has a unique solution in the quadrant $x, y \ge 0$ for any continuously differentiable boundary data on the lines $x = 0$, $y = 0$. When the boundary data are less regular, one has to consider the integrated form (35) of the equation instead. Note that $\mathbf{h}(x, 0)$ and $\mathbf{h}(0, y)$ must be 1-Lipschitz by the definition of the height function.

REMARK 5.3. In terms of the partial derivatives of $\mathbf{h}(x, y)$ and $\mathfrak{q}$, $\mathfrak{s}$ parameters, the equation (69) turns into a *nonlinear* PDE

$$\frac{1}{\ln(\mathfrak{q})}\mathbf{h}_{xy} + \mathbf{h}_x\mathbf{h}_y + \frac{1}{\mathfrak{s}-1}\mathbf{h}_x + \frac{\mathfrak{s}}{\mathfrak{s}-1}\mathbf{h}_y = 0. \tag{71}$$

In terms of $\rho = \mathbf{h}_x$ it gives (writing (71) as an expression of $\mathbf{h}_y$ through $\mathbf{h}_x$, $\mathbf{h}_{xy}$ and differentiating with respect to x)

$$\begin{aligned}\frac{1}{\ln(\mathfrak{q})}\left(\rho_{xy} + \frac{(1-\mathfrak{s})\rho_x\rho_y}{\mathfrak{s}+(\mathfrak{s}-1)\rho}\right) + \rho_x \cdot \frac{\mathfrak{s}}{\mathfrak{s}-1} \cdot \frac{1}{\mathfrak{s}+(\mathfrak{s}-1)\rho} \\ + \rho_y \cdot \frac{1}{\mathfrak{s}-1} \cdot \big(\mathfrak{s}+(\mathfrak{s}-1)\rho\big).\end{aligned} \tag{72}$$

As $\mathfrak{q} \to 0$, (72) becomes the equation for the limit shape of the stochastic six-vertex model discussed in [58], in agreement with Proposition 2.3 above.

Another limit is $\mathfrak{s} \to 1$ with fixed $\mathfrak{q}$, which turns (71) into $\mathbf{h}_x + \mathbf{h}_y = 0$. The limit shape $\mathbf{h}$ becomes constant along the lines $x - y = const$.

PROOF OF THEOREM 5.1. The function $\frac{1}{L}H(Lx, Ly)$ is monotone and 1-Lipschitz in each of its variables. Therefore, by the Arzela–Ascoli theorem, the sequence of functions $\mathbb{E}q^{H(Lx,Ly)}$ has subsequential limits (with respect to supremum norm topology on continuous functions in $[0,a] \times [0,b]$) which are also Lipschitz. Let $\tilde{\mathbf{h}}(x, y)$ be one of such limits. Taking the expectation of (34), we obtain

$$\begin{aligned}&-(1-b)\sum_{x=1}^{LX-1} \mathbb{E}q^{H(x,0)} - (1-bq)\sum_{y=1}^{LY-1} \mathbb{E}q^{H(0,y)} \\ &+ (1-b)\sum_{x=1}^{LX-1} \mathbb{E}q^{H(x,LY)} + (1-bq)\sum_{y=1}^{LY-1} \mathbb{E}q^{H(LX,y)} \\ &+ (b+bq-1)\mathbb{E}q^{H(0,0)} - bq \cdot \mathbb{E}q^{H(LX,0)} \\ &- b \cdot \mathbb{E}q^{H(0,LY)} + \mathbb{E}q^{H(LX,LY)} = 0.\end{aligned} \tag{73}$$

Sending $L \to \infty$ in (73), we get for all $0 \le X \le a$, $0 \le Y \le b$,

$$\begin{aligned}&-\beta \int_0^X \mathfrak{q}^{\tilde{\mathbf{h}}(x,0)}\,dx - \big(\beta - \ln(\mathfrak{q})\big)\int_0^Y \mathfrak{q}^{\tilde{\mathbf{h}}(0,y)}\,dy + \beta \int_0^X \mathfrak{q}^{\tilde{\mathbf{h}}(x,Y)}\,dx \\ &+ \big(\beta - \ln(\mathfrak{q})\big)\int_0^Y \mathfrak{q}^{\tilde{\mathbf{h}}(X,y)}\,dy - \mathfrak{q}^{\tilde{\mathbf{h}}(0,0)} - \mathfrak{q}^{\tilde{\mathbf{h}}(X,0)} - \mathfrak{q}^{\tilde{\mathbf{h}}(0,Y)} + \mathfrak{q}^{\tilde{\mathbf{h}}(X,Y)} = 0.\end{aligned} \tag{74}$$

By Proposition 4.1, the integral equation (74) has a unique solution. Hence, all limiting points $\tilde{\mathbf{h}}$ coincide with a unique limit $\mathbf{h}$, and $\mathfrak{q}^{\mathbf{h}}$ solves (69).

So far we have shown that the expectation $\mathbb{E}q^H$ converges to $\mathfrak{q}^{\mathbf{h}}$, and next we show that the fluctuations decay to 0.

Set $U(x,y)=q^{H(Lx,Ly)}-\mathbb{E}q^{H(Lx,Ly)}$. Subtracting (73) from (34), we obtain

$$\begin{aligned} &U(X,Y)+(1-b)\sum_{x=1}^{LX-1}U(x/L,Y)+(1-bq)\sum_{y=1}^{LY-1}U(X,y/L) \\ &\quad=\sum_{x=1}^{LX}\sum_{y=1}^{LY}\xi(x,y). \end{aligned} \tag{75}$$

We claim that the maximum of right-hand side of (75) over $(X,Y)\in[0,a]\times[0,b]$ converges to 0 in probability as $L\to\infty$. Indeed, consider the function

$$V(X,Y)=\sum_{x=1}^{LX}\sum_{y=1}^{LY}\xi(x,y).$$

Since $U(X,Y)$, $(X,Y)\in[0,a]\times[0,b]$, is Lipschitz, (75) implies that so is $V(X,Y)$. Thus, it suffices to show that for *some fixed* X and Y, $V(X,Y)\to 0$ in probability. Using (32) (see Remark 3.2), we get

$$\mathbb{E}[V(X,Y)]^2=\sum_{x=1}^{LX}\sum_{y=1}^{LY}\mathbb{E}[\xi(x,y)]^2 \tag{76}$$

We further use (33) to compute each term of the right-hand side. Note that $|\Delta_x|<C(1-q)$, $|\Delta_y|<C(1-q)$ for a constant $C>0$ which depends only on a,b. It follows that as $L\to\infty$, $\mathbb{E}[\xi(x,y)]^2\le \text{const}\cdot L^{-3}$ and (76) goes to 0 as $\text{const}\cdot L^{-1}$. Thus, $V(X,Y)$ converges to 0 in probability.

The uniformly bounded random functions $U(X,Y)$ are uniformly Lipschitz on $[0,a]\times[0,b]$ as $L\to\infty$. Therefore, their laws are tight (in Skorohod topology) as $L\to\infty$; see, for example, [38], Corollary 3.7.4. Any subsequential limit $\tilde{U}$ has continuous trajectories and must solve the $L=\infty$ version of (75), which reads

$$\begin{aligned} &\tilde{U}(X,Y)+\beta_1\int_0^X\tilde{U}(x,Y)\,dx+\beta_2\int_0^Y\tilde{U}(X,y)\,dy=0, \\ &0\le x,y\le M. \end{aligned} \tag{77}$$

By Proposition 4.1, the only solution to (77) is $\tilde{U}\equiv 0$. Thus, the law of $U(X,Y)$, $(X,Y)\in[0,a]\times[0,b]$, converges to the law of the zero function.

We have thus shown that $\sup_{(x,y)\in[0,a]\times[0,b]}|q^{H(Lx,Ly)}-\mathfrak{q}^{\mathbf{h}}(x,y)|\to 0$ in probability as $L\to\infty$, which implies (70). □

REMARK 5.4. An alternative way to prove Theorem 5.1 is to use Theorems 3.1 and 4.7 to represent q^H through the Riemann function. The convergence of the discrete Riemann function to its continuous counterpart of Theorem 4.4 would then imply the description of the limiting profile through the telegraph equation.

5.2. *Consistency check.* We would like to directly see that the result of Theorem 5.1 complemented with formulas for the solution of Theorem 4.4 matches the contour integral expression of Theorem 2.1 at $\alpha = 0$.

Let us find formulas for the solution to (40) with specific boundary condition. We take $u(X,Y) = 0$, $\phi(X,0) = \mathfrak{q}^{-p_1 X} = \exp(-(\beta_1-\beta_2)p_1 X)$, $\phi(0,Y) = \mathfrak{q}^{p_2 Y} = \exp((\beta_1-\beta_2)p_2 Y)$ for two constants p_1, p_2. Then the solution is

$$
\begin{aligned}
&2\pi\mathbf{i}\phi(X,Y)\\
&\quad = 2\pi\mathbf{i}\mathcal{R}(X,Y;0,0)\\
&\qquad + 2\pi\mathbf{i}\int_0^Y \mathcal{R}(X,Y;0,y)\big(p_2(\beta_1-\beta_2)+\beta_2\big)\exp\big((\beta_1-\beta_2)p_2 y\big)\,dy\\
&\qquad + 2\pi\mathbf{i}\int_0^X \mathcal{R}(X,Y;x,0)\big(-p_1(\beta_1-\beta_2)+\beta_1\big)\exp\big(-(\beta_1-\beta_2)p_1 x\big)\,dx.
\end{aligned}
\tag{78}
$$

Plugging in the definition of $\mathcal{R}$ and integrating in x and y, this can be transformed to (with the notation $p_i = \frac{\rho_i}{1+\rho_i}$, so that $\rho_i = \frac{p_i}{1-p_i}$)

$$
\begin{aligned}
&\oint_{-\beta_1} \exp\left[(\beta_1-\beta_2)\left(-X\frac{z}{z+\beta_2} + Y\frac{z}{z+\beta_1}\right)\right]\frac{(\beta_2\rho_1-\beta_1\rho_2)\,dz}{(z-\beta_1\rho_2)(z-\beta_2\rho_1)}\\
&\quad - \oint_{-\beta_1} \frac{\rho_1\beta_2+\beta_1}{z-\rho_1\beta_2}\exp\left[(\beta_1-\beta_2)Y\frac{z}{z+\beta_1}\right]\\
&\quad \times\left(\exp\left[-\frac{\rho_1}{1+\rho_1}(\beta_1-\beta_2)X\right]\right)\frac{dz}{(z+\beta_1)}.
\end{aligned}
\tag{79}
$$

Note that the residue at $z = \rho_1\beta_2$ for both terms in (79) coincides with

$$
\exp\left[(\beta_1-\beta_2)\left(-X\frac{\rho_1}{1+\rho_1} + Y\frac{\rho_1\beta_2}{\rho_1\beta_2+\beta_1}\right)\right].
$$

Thus, we can include $\rho_1\beta_2$ into the integration contours. After that, the second integral vanishes, and we get the final expression

$$
\oint_{-\beta_1,\rho_1\beta_2} \exp\left[(\beta_1-\beta_2)\left(-X\frac{z}{z+\beta_2} + Y\frac{z}{z+\beta_1}\right)\right]\frac{(\beta_2\rho_1-\beta_1\rho_2)\,dz}{(z-\beta_1\rho_2)(z-\beta_2\rho_1)}.
\tag{80}
$$

In particular, when $p_1 = 0$, $p_2 = 1$ (i.e., $\rho_1 = 0$, $\rho_2 = +\infty$), we return to the domain wall boundary conditions, and the contour integral transforms into

$$
\oint_{-\beta_1,0} \exp\left[(\beta_1-\beta_2)\left(-X\frac{z}{z+\beta_2} + Y\frac{z}{z+\beta_1}\right)\right]\frac{dz}{z},
\tag{81}
$$

in agreement with Theorem 2.1 (cf. Remark 2.2). Note that 0 is included in the contour, as here we deal with $\mathfrak{q}^{\mathbf{h}(x,y)}$, while (7) corresponded to $\mathfrak{q}^{\mathbf{h}(x,y)} - 1$.

6. CLT for general boundary conditions. We say that a function $f : [a, b] \to \mathbb{R}$ is piecewise C^1-smooth, if it is continuous on the segment $[a, b]$ and there exists a finite partition $a = x_0 < x_1 < \cdots < x_n = b$ such that f is continuously differentiable on each open interval (x_{i-1}, x_i), $1 \le i \le n$, and its derivative has left and right limits at each point x_i, $1 \le i \le n-1$.

The goal of this section is to prove the following statement.

THEOREM 6.1. *In the setting of Theorem 5.1, assume additionally that the boundary conditions $\chi(x)$, $\psi(y)$ are piecewise C^1-smooth.*[5] *Then the fluctuation field $\sqrt{L}(q^{H(Lx,Ly)} - \mathbb{E}q^{H(Lx,Ly)})$ converges as $L \to \infty$ (in the sense of convergence of finite-dimensional distributions) to a random Gaussian field $\phi(x, y)$, $x, y \ge 0$, which solves*

$$\begin{aligned}\phi_{xy} &+ \beta_1\phi_y + \beta_2\phi_x \\ &= \eta \cdot \sqrt{(\beta_1 + \beta_2)\mathfrak{q}^{\mathbf{h}}_x\mathfrak{q}^{\mathbf{h}}_y + (\beta_2 - \beta_1)\beta_2\mathfrak{q}^{\mathbf{h}}\mathfrak{q}^{\mathbf{h}}_x - (\beta_2 - \beta_1)\beta_1\mathfrak{q}^{\mathbf{h}}\mathfrak{q}^{\mathbf{h}}_y}\end{aligned} \tag{82}$$

with zero boundary conditions $\phi(x, 0) = \phi(0, y) = 0$, where η is the two-dimensional white noise, and $\mathfrak{q}^{\mathbf{h}}$ is the limit shape afforded by Theorem 5.1.

REMARK 6.2. The first version of this text stated Theorem 6.1 as a conjecture; we also provided two heuristic arguments for it. The conjecture was proved by Shen and Tsai a few months later; see [61]. On the other hand, we later realized that one of our heuristic arguments could be also turned into a complete proof (different from the one in [61]); it is this proof that we include below. Our other heuristic argument can be found in the Appendix.

REMARK 6.3. There are two ways to make sense of the solution to (82). One can use the integrated form (35) to smooth out the white noise. Alternatively, one can use the formula for the solution of Theorem 4.4.

REMARK 6.4. If we denote $\phi(x, y) = \psi(x, y)\mathfrak{q}^{\mathbf{h}(x,y)} \ln(\mathfrak{q})$, so that

$$\psi(x, y) = \lim_{L\to\infty} \frac{H(Lx, Ly) - \mathbb{E}H(Lx, Ly)}{\sqrt{L}},$$

then (82) is rewritten as

$$\begin{aligned}\psi_{xy} &+ \beta_1\psi_y + \beta_2\psi_x + (\beta_1 - \beta_2)(\psi_y\mathbf{h}_x + \psi_x\mathbf{h}_y) \\ &= \eta \cdot \sqrt{(\beta_1 + \beta_2)\mathbf{h}_x\mathbf{h}_y - \beta_2\mathbf{h}_x + \beta_1\mathbf{h}_y}.\end{aligned} \tag{83}$$

[5] We believe that the statement is true for arbitrary monotone and 1-Lipschitz χ and ψ. However, without the piecewise-smoothness condition the justification of convergence of the sum (96) to the integral (97) needs additional technical efforts.

REMARK 6.5. We checked on a computer the consistency between (82) and Theorem 2.4. Namely, using Theorem 4.4, the solution to (40) has the covariance

$$\begin{aligned}&\operatorname{Cov}(\phi(X_1,Y_1),\phi(X_2,Y_2))\\&\quad=\int_0^{X_1\wedge X_2}\int_0^{Y_1\wedge Y_2}\mathcal{R}(X_1,Y_1;x,y)\mathcal{R}(X_2,Y_2;x,y)V^{\infty}(x,y)\,dx\,dy,\end{aligned}\tag{84}$$

with V^{∞} as in the second line of (97) below. Plugging into (84), the contour integral expressions for $\mathcal{R}$ and the expressions for $\mathfrak{q}^{\mathbf{h}}$ of Theorem 2.1 for the domain wall boundary conditions we arrive at a 6-fold integral expression. On the other hand, it has to be equal to the double contour integral of Theorem 2.4 (for points on the same horizontal line, as in that theorem). We actually do not know how to verify it rigorously without using Theorem 6.1, but evaluation of both expressions using Maple software (using symbolic computations of terms for converging series) shows that they are indeed equal.

In the rest of this section, we prove Theorem 6.1. The idea is to combine Theorems 3.1 and 4.7 with martingale central limit theorem to reach the result. We detail only one-point convergence, as convergence of finite-dimensional distributions is proven in the same way by invoking multi-dimensional CLT instead of its one-dimensional counterpart.

We combine Theorem 3.1 with Theorem 4.7 to get

$$\begin{aligned}q^{H(X,Y)}=q^{H(0,0)}&\mathcal{R}^d(X,Y;0,0)\\&+\sum_{y=1}^{Y}\mathcal{R}^d(X,Y;0,y)\big(q^{H(0,y)}-b_2q^{H(0,y-1)}\big)\\&+\sum_{x=1}^{X}\mathcal{R}^d(X,Y;x,0)\big(q^{H(x,0)}-b_1q^{H(x-1,0)}\big)\\&+\sum_{x=1}^{X}\sum_{y=1}^{Y}\mathcal{R}^d(X,Y;x,y)\xi(x,y).\end{aligned}\tag{85}$$

The first three terms in (85) are deterministic, while the expectation of $\xi(x,y)$ vanishes. Therefore, rescaling $(X,Y)\mapsto(LX,LY)$, we get

$$q^{H(LX,LY)}-\mathbb{E}q^{H(LX,LY)}=\sum_{x=1}^{LX}\sum_{y=1}^{LY}\mathcal{R}^d(LX,LY;x,y)\xi(x,y).\tag{86}$$

We now compute the $L\to\infty$ limit of the variance of (86). Relation (32) implies that $\xi(x,y)$ is uncorrelated noise; denote its variance by $V(x,y)$. Then

$$\mathbb{E}\big(q^{H(LX,LY)}-\mathbb{E}q^{H(LX,LY)}\big)^2=\mathbb{E}\Bigg[\sum_{x=1}^{LX}\sum_{y=1}^{LY}\big[\mathcal{R}^d(LX,LY;x,y)\big]^2V(x,y)\Bigg].\tag{87}$$

$V(x, y)$ is computed through (33) to be

$$V(x, y) = \big(qb(1-b) + b(1-qb)\big)\Delta_x\Delta_y \\ + b(1-qb)(1-q)q^{H(x,y)}\Delta_x - b(1-b)(1-q)q^{H(x,y)}\Delta_y. \tag{88}$$

Choose a small parameter $\theta > 0$. We split the summation domain $[1, LX] \times [1, LY]$ in (87) into disjoint squares of size $\theta L \times \theta L$ (and possibly smaller rectangles near the boundary of the domain). Take one such square $[LX_0, LX_0 + L\theta] \times [LY_0, LY_0 + L\theta]$ and consider the part of the sum corresponding to the indices x and y inside it. We first approximate the sum in the right-hand side of (87) without expectation and then take the expectation at the last step. Note that $|V(x, y)| < \text{const} \cdot L^{-3}$, since $1-b$, $1-qb$, $1-q$, Δ_x and Δ_y all decay as L^{-1}. Therefore, the random variable under expectation in (87) multiplied by L is uniformly bounded. Hence, convergence in probability would imply convergence of expectation in (87).

Let us deal with the terms in the second line of (88) and concentrate on $b(1-qb)(1-q)[q^{H(x,y)}\Delta_x]$. Since $H(x, y)$ is 1-Lipschitz in both variables, using Theorem 5.1, we get

$$q^{H(x,y)} = q^{H(LX_0,LY_0)} + O(\theta) = \mathfrak{q}^{\mathbf{h}(X_0,Y_0)} + o(1) + O(\theta),$$

where the remainder $o(1)$ tends to 0 in probability as $L \to \infty$ uniformly in $(x, y) \in [1, LX] \times [1, LY]$, and remainder $O(\theta)$ is bounded from above by a deterministic constant tending to zero with speed θ as $\theta \to 0$. Also

$$\big[\mathcal{R}^d(LX, LY; x, y)\big]^2 = \big[\mathcal{R}(X, Y; X_0, Y_0)\big]^2 + O(\theta).$$

Without loss of generality, we may assume that $q < 1$. Then Δ_x is a *positive number*, hence summations of $(o(1) + O(\theta)) \cdot \Delta_x$ cause no problems: if real numbers $a_1, a_1, \dots, a_k$ are positive and real numbers $e_1, \dots, e_k$ satisfy $|e_i| < C$, then $|a_1e_1 + a_2e_2 + \cdots + a_ke_k| \le C(a_1 + \cdots + a_k)$. We conclude that

$$\sum_{\substack{x\in[LX_0,LX_0+L\theta]\\ y\in[LY_0,LY_0+L\theta]}} \big[\mathcal{R}^d(LX, LY; x, y)\big]^2 b(1-qb)(1-q)q^{H(x,y)}\Delta_x \\ = -L^{-2}\beta_2\ln(\mathfrak{q})\big[\mathcal{R}(X, Y; X_0, Y_0)\big]^2\mathfrak{q}^{\mathbf{h}(X_0,Y_0)} \\ \times\Bigg(\sum_{y\in[LY_0,LY_0+L\theta]}\big(q^{H(LX_0+L\theta+1,y)} - q^{H(LX_0,y)}\big)\Bigg) \\ + \big(o(1) + O(\theta)\big)\cdot L^{-2}\cdot(\theta L)\cdot\sup_y\big(q^{H(LX_0+L\theta+1,y)} - q^{H(LX_0,y)}\big). \tag{89}$$

Applying Theorem 5.1 again, we get

$$-\theta L^{-1}\beta_2\ln(\mathfrak{q})\big[\mathcal{R}(X, Y; X_0, Y_0)\big]^2\mathfrak{q}^{\mathbf{h}(X_0,Y_0)}\big(\mathfrak{q}^{\mathbf{h}(X_0+\theta,Y_0)} - \mathfrak{q}^{\mathbf{h}(X_0,Y_0)}\big) \\ + \theta L^{-1}o(1) + \big(o(1) + O(\theta)\big)L^{-1}\theta^2. \tag{90}$$

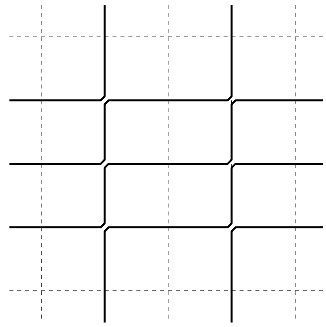

FIG. 6. *When there are no corner-type vertices* (*types V and VI*), *the configuration of the six-vertex model looks like a grid with the number of intersections* (*i.e., type II vertices*) *equal to the product of the numbers of vertically and horizontally incoming paths*. $6 = 2 \times 3$ *in the picture.*

Similarly, the asymptotic behavior of the sum of the terms arising from $-b(1-b)(1-q)q^{H(x,y)}\Delta_y$ in the third line of (88) is

$$\begin{aligned}(91)\qquad &\theta L^{-1}\beta_1 \ln(\mathfrak{q})\big[\mathcal{R}(X,Y;X_0,Y_0)\big]^2 \mathfrak{q}^{\mathbf{h}(X_0,Y_0)}\big(\mathfrak{q}^{\mathbf{h}(X_0,Y_0+\theta)} - \mathfrak{q}^{\mathbf{h}(X_0,Y_0)}\big)\\ &\quad + \theta L^{-1} o(1) + \big(o(1)+O(\theta)\big)L^{-1}\theta^2.\end{aligned}$$

The next step is to deal with the first line of (88), which is more complicated due to the product $\Delta_x\Delta_y$. The key observation here is that the random variable $\Delta_x\Delta_y$ vanishes unless the vertex at $(x+1, y+1)$ has type *II*, as in Figure 3; in the latter case, $\Delta_x\Delta_y$ is $q^{2H(x,y)}(1-q)(1-q^{-1})$. Arguing similarly to the previous two cases, we then write

$$\begin{aligned}&\sum_{\substack{x\in[LX_0,LX_0+L\theta]\\ y\in[LY_0,LY_0+L\theta]}} \big[\mathcal{R}^d(LX,LY;x,y)\big]^2\big(qb(1-b)+b(1-qb)\big)\Delta_x\Delta_y\\ (92)\qquad &\quad = \big(o(1)+O(\theta)\big)\cdot L^{-1}\cdot\theta^2\\ &\qquad - L^{-3}\big[\mathcal{R}(X,Y;X_0,Y_0)\big]^2(\beta_1+\beta_1)\ln^2(\mathfrak{q})\mathfrak{q}^{2\mathbf{h}(X_0,Y_0)}\\ &\qquad \times \#\big\{\text{type } II \text{ vertices in } [LX_0, LX_0+L\theta]\times[LY_0,LY_0+L\theta]\big\}.\end{aligned}$$

We would like to understand the last line of (92). For that, let $\square$ denote the square $[LX_0, LX_0+L\theta]\times[LY_0, LY_0+L\theta]$. Suppose that along the bottom part of $\square$, n paths are entering inside it, and along the left part of $\square$, m paths are entering inside. Further, suppose that there are $\mathcal{C}$ vertices of types V and VI inside $\square$—these vertices represent "corners." Note that if $\mathcal{C}=0$, then the number of type *II* vertices in $\square$ is $n\cdot m$. Indeed, if we reinterpret the type *II* vertex as two paths transversally intersecting each other (rather than touching), then each of n paths which entered vertically, must intersect each of the m paths which entered horizontally; cf. Figure 6. Let us view the general $\mathcal{C}>0$ case as a perturbation of $\mathcal{C}=0$.

Then each of $\mathcal{C}$ corners might change the number of type *II* vertices at most by θL, as adding this corner changes the behavior of only one path. The conclusion is that

$$\big|(\text{Number of type } II \text{ vertices in } \square) - nm\big| \le \theta L \cdot \mathcal{C}. \tag{93}$$

Let us now find an upper bound for $\mathcal{C}$. Let U be the sum of $\theta^2 L^2$ i.i.d. Bernoulli random variables ξ_i with $\mathrm{Prob}(\xi_i = 1) = 1 - \min(b_1, b_2)$, $\mathrm{Prob}(\xi_i = 0) = \min(b_1, b_2)$. Then the definition of the stochastic six-vertex model implies that $\mathcal{C} \le U$ in the sense of stochastic dominance. In particular, $\mathbb{E}\mathcal{C} \le \text{const} \cdot \frac{\theta^2 L^2}{L}$, and $\mathcal{C} \le \text{const} \cdot \frac{\theta^2 L^2}{L}$ with probability tending to 1 as $L \to \infty$.

We conclude that

$$\big|(\text{Number of type } II \text{ vertices in } \square) - nm\big| \le \text{const} \cdot \theta^3 L^2 \tag{94}$$

both in expectation and with high probability as $L \to \infty$. Finally,

$$\begin{aligned} n &= H(LX_0, LY_0) - H(LX_0 + L\theta, LY_0) \\ &= L\big(\mathbf{h}(X_0, Y_0) - \mathbf{h}(X_0 + \theta, Y_0)\big) + L \cdot o(1), \\ m &= L\big(\mathbf{h}(X_0, Y_0 + \theta) - \mathbf{h}(X_0, Y_0)\big) + L \cdot o(1), \end{aligned}$$

and (92) turns into

$$\begin{aligned} & o(1) \cdot L^{-1} + O(\theta^3) \cdot L^{-1} \\ & \quad + L^{-1}\big[\mathcal{R}(X, Y; X_0, Y_0)\big]^2 (\beta_1 + \beta_1) \ln^2(\mathfrak{q}) \mathfrak{q}^{2\mathbf{h}(X_0, Y_0)} \\ & \quad \times \big(\mathbf{h}(X_0 + \theta, Y_0) - \mathbf{h}(X_0, Y_0)\big) \cdot \big(\mathbf{h}(X_0, Y_0 + \theta) - \mathbf{h}(X_0, Y_0)\big). \end{aligned} \tag{95}$$

We now combine the terms from (90), (91), (95) and obtain

$$\begin{aligned} & L\left[\sum_{x=1}^{LX} \sum_{y=1}^{LY} \big[\mathcal{R}^d(LX, LY; x, y)\big]^2 V(x, y)\right] \\ & \quad = \sum_{0 \le i \le X/\theta} \sum_{0 \le j \le Y/\theta} \big[\mathcal{R}(X, Y; \theta i, \theta j)\big]^2 \big[-\theta\beta_2 \ln(\mathfrak{q}) \mathfrak{q}^{\mathbf{h}(\theta i, \theta j)} \\ & \qquad \times \big(\mathfrak{q}^{\mathbf{h}(\theta(i+1), \theta j)} - \mathfrak{q}^{\mathbf{h}(\theta i, \theta j)}\big) \\ & \qquad + \theta\beta_1 \ln(\mathfrak{q}) \mathfrak{q}^{\mathbf{h}(\theta i, \theta j)} \big(\mathfrak{q}^{\mathbf{h}(\theta i, \theta(j+1))} - \mathfrak{q}^{\mathbf{h}(\theta i, \theta j)}\big) \\ & \qquad + (\beta_1 + \beta_1) \ln^2(\mathfrak{q}) \mathfrak{q}^{2\mathbf{h}(\theta i, \theta j)} \big(\mathbf{h}\big(\theta(i+1), \theta j\big) \\ & \qquad - \mathbf{h}(\theta i, \theta j)\big) \cdot \big(\mathbf{h}\big(\theta i, \theta(j+1)\big) - \mathbf{h}(\theta i, \theta j)\big)\big] \\ & \qquad + o(1) + O(\theta), \end{aligned} \tag{96}$$

where $o(1)$ is a random term which (for any fixed $\theta > 0$) converges to 0 in probability as $L \to \infty$, and $O(\theta)$ is a θ-dependent random variable, whose absolute value is almost surely bounded by $\text{const} \cdot \theta$.

At this point, we first send $L \to \infty$ and then $\theta \to 0$. Note that the sum in the right-hand side of (96) is deterministic, so there is no randomness involved in the $\theta \to 0$ limit. Recall that $\mathfrak{q}^{\mathbf{h}}$ solves the telegraph equation (69). The boundary data $\chi(x)$, $\psi(y)$ are two piecewise C^1-smooth functions. Hence, due to integral representation of the solution (42), $\mathfrak{q}^{\mathbf{h}}$ and, therefore, also $\mathbf{h}$ inherit smoothness: $\mathbf{h}_x$ is piecewise-continuous in x and continuous in y; $\mathbf{h}_y$ is continuous in x and piecewise-continuous in x. Hence, all the terms in (96) are smooth and as $\theta \to 0$ the sum converges to an integral. We conclude that

$$\lim_{L\to\infty} L\Bigg[\sum_{x=1}^{LX}\sum_{y=1}^{LY}\big[\mathcal{R}^d(LX, LY; x, y)\big]^2 V(x, y)\Bigg]$$

$$(97)\quad = \int_0^X \int_0^Y dx\, dy\big[\mathcal{R}(X, Y; x, y)\big]^2\big[-\beta_2 \ln(\mathfrak{q})\mathfrak{q}^{\mathbf{h}(x,y)}\mathfrak{q}_x^{\mathbf{h}(x,y)} + \beta_1 \ln(\mathfrak{q})\mathfrak{q}^{\mathbf{h}(x,y)}\mathfrak{q}_y^{\mathbf{h}(x,y)} + (\beta_1+\beta_1)\ln^2(\mathfrak{q})\mathfrak{q}^{2\mathbf{h}(x,y)}\mathbf{h}_x(x, y)\mathbf{h}_y(x, y)\big],$$

both in probability and in expectation. Since $\ln(\mathfrak{q}) = \beta_1 - \beta_2$ and $\mathfrak{q}_x^{\mathbf{h}} = \ln(\mathfrak{q})\mathfrak{q}_x^{\mathbf{h}}$, $\mathfrak{q}_y^{\mathbf{h}} = \ln(\mathfrak{q})\mathfrak{q}^{\mathbf{h}}\mathbf{h}_y$, (97) matches the variance of the solution to (82) at point (X, Y) when written in the form of Theorem 4.4.

If instead of variance, we compute the $L \to \infty$ limit of the covariance of (86) at $(X, Y) = (X_1, Y_1)$ and $(X, Y) = (X_2, Y_2)$, then the argument is very similar. Indeed, since the noise $\xi(x, y)$ is uncorrelated, (87) is replaced with

$$\mathbb{E}\big[\big(q^{H(LX_1,LY_1)} - \mathbb{E}q^{H(LX_1,LY_1)}\big)\big(q^{H(LX_2,LY_2)} - \mathbb{E}q^{H(LX_2,LY_2)}\big)\big]$$

$$(98)\quad = \mathbb{E}\Bigg[\sum_{x=1}^{L\min(X_1,X_2)}\sum_{y=1}^{L\min(Y_1,Y_2)} \mathcal{R}^d(LX_1, LY_1; x, y) \times \mathcal{R}^d(LX_2, LY_2; x, y)V(x, y)\Bigg].$$

Repeating the asymptotic analysis of (87), we arrive at an analogue of (97):

$$\lim_{L\to\infty} L\Bigg[\sum_{x=1}^{L\min(X_1,X_2)}\sum_{y=1}^{L\min(Y_1,Y_2)} \mathcal{R}^d(LX_1, LY_1; x, y)\mathcal{R}^d(LX_2, LY_2; x, y)V(x, y)\Bigg]$$

$$= \int_0^{\min(X_1,X_2)}\int_0^{\min(Y_1,Y_2)} dx\, dy \mathcal{R}(X_1, Y_1; x, y)\mathcal{R}(X_2, Y_2; x, y) \times \big[-\beta_2 \ln(\mathfrak{q})\mathfrak{q}^{\mathbf{h}(x,x)}\mathfrak{q}_x^{\mathbf{h}(x,y)} + \beta_1 \ln(\mathfrak{q})\mathfrak{q}^{\mathbf{h}(x,y)}\mathfrak{q}_y^{\mathbf{h}(x,y)} + (\beta_1+\beta_1)\ln^2(\mathfrak{q})\mathfrak{q}^{2\mathbf{h}(x,y)}\mathbf{h}_x(x, y)\mathbf{h}_y(x, y)\big],$$

which matches the covariance of the solution to (82) at points (X_1, Y_1) and (X_2, Y_2) when written in the form of Theorem 4.4.

It remains to prove the asymptotic Gaussianity of (86). Let us linearly order the integer points inside the rectangle $[1, LX] \times [1, LY]$ as follows: $(1, 1)$, $(2, 1)$, $(1, 2)$, $(3, 1)$, $(2, 2)$, $(1, 3)$, $(4, 1)$, $(3, 2)$, $(2, 3)$, $(1, 4), \dots,$ that is, we sequentially trace the diagonals $x + y = \text{const}$. Theorem 3.1 implies that then $\mathcal{R}^d(LX, LY; x, y)\xi(x, y)$ is a martingale difference in (x, y), and we can apply the martingale central limit theorem; see, for example, [42], Section 3. There are two conditions to check:

1. The conditional variance, which by Theorem 3.1 is given by

$$\sum_{x=1}^{LX}\sum_{y=1}^{LY}[\mathcal{R}^d(LX, LY; x, y)]^2 V(x, y),$$

with V as in (88), should have the same $L \to \infty$ behavior as the unconditional variance (87), in the sense that the ratio tends to 1 in probability.

2. The Lindeberg condition should hold, which in our setting reads

$$\lim_{L\to\infty}\sum_{x=1}^{LX}\sum_{y=1}^{LY}\mathbb{E}\big[L \cdot \xi^2(x, y) I_{L\cdot\xi^2(x,y)>\varepsilon}\big] = 0 \quad \text{for each } \varepsilon > 0. \tag{99}$$

The first condition is a reformulation of (97) and, therefore, it is already proven. For the Lindeberg condition, note that by its definition (31), $|\xi(x, y)|$ is uniformly bounded by C/L for a deterministic constant C. Thus, the indicator $I_{\xi^2(x,y)L>\varepsilon}$ becomes empty as $L \to \infty$, and the expression (99) vanishes for large L. The asymptotic Gaussianity follows, and the proof of Theorem 6.1 is complete.

7. Low density limit. The law of large numbers of Section 5 and the central limit theorem of Section 6 admit a low density degeneration in which the asymptotic equations become *linear*. The degeneration is explained in this section.

We still work in the asymptotic regime (4), but we change the asymptotic behavior of the boundary conditions $H(x, 0)$ and $H(0, y)$, as compared to Theorems 5.1 and 6.1. We introduce a new parameter $0 < \delta < 1$ and assume that $H(Lx, 0)$ and $H(0, Ly)$ grow proportionally to $L^{1-\delta}$. This means that there are much fewer paths entering the quadrant from the bottom and from the left. Hence, the density of lines everywhere in the quadrant would stay low and tend to 0 as $L \to \infty$.

THEOREM 7.1. *Fix $a, b > 0$, and $0 < \delta < 1$. Take two continuous monotone functions $\chi : [0, a] \to \mathbb{R}$, $\psi : [0, b] \to \mathbb{R}$ such that $\chi(0) = \psi(0)$. Suppose that the boundary condition in the stochastic six-vertex model is chosen so that as $L \to \infty$, $L^{\delta-1}H(Lx, 0) \to \chi(x)$ and $L^{\delta-1}H(0, Lx) \to \psi(y)$ uniformly on $(x, y) \in [0, a] \times [0, b]$.*

Define the function $\mathbf{h} : [0, a] \times [0, b] \to \mathbb{R}$ as the solution to the PDE

$$\mathbf{h}_{xy} + \beta_2\mathbf{h}_x + \beta_1\mathbf{h}_y = 0, \quad x, y \geq 0; \qquad \mathbf{h}(x, 0) = \chi(x, 0), \qquad \mathbf{h}(0, y) = \psi(y, 0), \tag{100}$$

and a random field $\phi : [0, a] \times [0, b] \to \mathbb{R}$ *as a solution to*

$$\phi_{xy} + \beta_1 \phi_y + \beta_2 \phi_x = \eta \cdot \sqrt{\beta_1 \mathbf{h}_y - \beta_2 \mathbf{h}_x} \tag{101}$$

with zero boundary conditions $\phi(x, 0) = \phi(0, y) = 0$, *where* η *is the two-dimensional white noise. Then the height function* $H(x, y)$ *of the stochastic six-vertex model* ($\alpha = 0$) *satisfies* (*for* $(x, y) \in [0, a] \times [0, b]$)

$$\lim_{L\to\infty} \mathbb{E} \frac{H(Lx, Ly)}{L^{1-\delta}} = \mathbf{h}(x, y), \tag{102}$$

$$\lim_{L\to\infty} \frac{H(Lx, Ly) - \mathbb{E}H(Lx, Ly)}{\sqrt{L^{1-\delta}}} = \phi(x, y). \tag{103}$$

Let us present an interpretation of Theorem 7.1. Consider a $L^{1-\delta} \times L^{1-\delta}$ box inside $[1, LX] \times [1, LY]$. The height function $H(x, y)$ changes by a constant when we cross the box and, therefore, there are finitely many paths inside. Each path has rare turns and, as $L \to \infty$, it turns into a *persistent Poisson random walk*:

- Whenever a path travels to the right, it turns upwards with intensity β_1,
- whenever a path travels upwards, it turns to the right with intensity β_2.

Recall that the paths were interacting with each other through the nonintersecting condition. Let us now change the way we view the vertices of type V of Figure 3: instead of thinking that paths touch each other, let us imagine that we observe an *intersection* of vertical and horizontal paths. Now paths simply do not feel each other; the only interaction is that whenever paths intersect, they cannot turn at exactly the same moment. However, since intersections are rare, this interaction is negligible as $L \to \infty$. We conclude that in a $L^{1-\delta} \times L^{1-\delta}$ box the configuration as $L \to \infty$ is probabilistically indistinguishable from a collection of *independent* persistent Poisson random walks. Gluing together all $L^{1-\delta} \times L^{1-\delta}$ boxes, we conclude that the entire configuration in $[1, LX] \times [1, LY]$ looks like that.

Thus, Theorem 7.1 can be treated as the law of large numbers and central limit theorem for the height function of a collection of independent persistent Poisson random walks with prescribed densities of entry points on the boundary of the quadrant. We find it somewhat surprising that the stochastic PDE (101) appears in such a simple setup. It should be possible to prove this Poisson result directly without appealing to the discretization provided by the six-vertex model, but we leave this question out of the scope of the article.

The proof of Theorem 7.1 is similar to those of Theorems 5.1, 6.1. The details are presented in the Appendix.

APPENDIX A: PROOF OF THEOREM 7.1

Theorem 3.1 written in terms of $q^H - 1$ and combined with Theorem 4.7 implies that

$$\begin{aligned} q^{H(X,Y)} - 1 = {} & \sum_{y=1}^{Y} \mathcal{R}^d(X,Y;0,y)\big[\big(q^{H(0,y)}-1\big) - b_2\big(q^{H(0,y-1)}-1\big)\big] \\ & + \sum_{x=1}^{X} \mathcal{R}^d(X,Y;x,0)\big[\big(q^{H(x,0)}-1\big) - b_1\big(q^{H(x-1,0)}-1\big)\big] \\ & + \sum_{x=1}^{X}\sum_{y=1}^{Y} \mathcal{R}^d(X,Y;x,y)\xi(x,y). \end{aligned} \tag{104}$$

The first two terms of the right-hand side of (104) are deterministic and give $\mathbb{E}(q^H - 1)$, while the third one is responsible for the fluctuations. Resuming (104) and using $q^{H(0,0)} = 1$, we obtain

$$\begin{aligned} & \mathbb{E}\big[q^{H(X,Y)} - 1\big] \\ & \quad = \mathcal{R}^d(X,Y;0,Y)\big(q^{H(0,Y)}-1\big) \\ & \quad + \sum_{y=1}^{Y-1}\big[\mathcal{R}^d(X,Y;0,y) - b_2\mathcal{R}^d(X,Y;0,y+1)\big]\big(q^{H(0,y)}-1\big) \\ & \quad + \mathcal{R}^d(X,Y;X,0)\big(q^{H(X,0)}-1\big) \\ & \quad + \sum_{x=1}^{X-1}\big[\mathcal{R}^d(X,Y;x,0) - b_1\mathcal{R}^d(X,Y;x+1,0)\big]\big(q^{H(x,0)}-1\big). \end{aligned} \tag{105}$$

We now pass to the limit $L \to \infty$ in (105). For that, note the deterministic inequality

$$\big|H(x,y)\big| \le \big|H(La,0)\big| + \big|H(0,Lb)\big|, \quad 0 \le x \le La, 0 \le x \le Lb,$$

which implies

$$\begin{aligned} q^{H(x,y)} - 1 &= \ln(q)H(x,y) + O\big(\big[\ln(q)H(x,y)\big]^2\big) \\ &= \ln(q)H(x,y) + O\big(L^{-2\delta}\big). \end{aligned} \tag{106}$$

In addition, with the notation of Section 4,

$$\begin{aligned} & \lim_{L\to\infty} \mathcal{R}^d(LX,LY;Lx,Ly) = \mathcal{R}(X,Y;x,y), \\ & \lim_{L\to\infty} L\big(\mathcal{R}^d(LX,LY;Lx,Ly) - b_2\mathcal{R}^d(LX,LY;Lx,Ly+1)\big) \\ & \quad = \beta_2\mathcal{R}(X,Y;x,y) - \mathcal{R}_y(X,Y;x,y), \end{aligned}$$

$$\lim_{L\to\infty} L\big(\mathcal{R}^d(LX,LY;Lx,Ly)-b_1\mathcal{R}^d(LX,LY;Lx+1,Ly)\big)$$
$$=\beta_1\mathcal{R}(X,Y;x,y)-\mathcal{R}_x(X,Y;x,y).$$

We conclude that

$$\begin{aligned}\lim_{L\to\infty}\mathbb{E}\frac{H(LX,LY)}{L^{1-\delta}}&\\ &=\mathcal{R}(X,Y;0,Y)\mathbf{h}(0,Y)\\ &\quad+\int_0^Y[\beta_2\mathcal{R}(X,Y;0,y)-\mathcal{R}_y(X,Y;0,y)]\mathbf{h}(0,y)\,dy\\ &\quad+\mathcal{R}(X,Y;X,0)\mathbf{h}(X,0)\\ &\quad+\int_0^X[\beta_1\mathcal{R}(X,Y;x,0)-\mathcal{R}_x(X,Y;x,0)]\mathbf{h}(x,0)\,dx.\end{aligned}\tag{107}$$

When integrated by parts, (107) matches the formula of Theorem 4.4 for the solution to (100).

Thus, (102) is proved and we proceed to (103). Using (104), we have

$$q^{H(LX,LY)}-\mathbb{E}q^{H(LX,LY)}=\sum_{x=1}^{LX}\sum_{y=1}^{LY}\mathcal{R}^d(LX,LY;x,y)\xi(x,y).\tag{108}$$

The remaining proof proceeds in the following two steps: we first show that the finite-dimensional distributions of (108) converge to those of the Gaussian process $(\beta_1-\beta_2)\phi(X,Y)$, and then deduce the limit for the centered height function $H(LX,LY)$ as a corollary. In fact, in the first step we will detail only one-point convergence; the convergence of any finite-dimensional distributions is proven in the same way by invoking the multidimensional central limit theorem instead of the one-dimensional version (cf. the proof of Theorem 6.1 above).

Let us investigate the variance of the right-hand side of (108) as $L\to\infty$. From (32), (33) the variance equals

$$\begin{aligned}&\sum_{x=1}^{LX}\sum_{y=1}^{LY}\mathcal{R}^d(LX,LY;x,y)^2\\ &\quad\times\mathbb{E}\big[\big(qb(1-b)+b(1-qb)\big)\big(q^{H(x,y)}-q^{H(x-1,y)}\big)\\ &\quad\times\big(q^{H(x,y)}-q^{H(x,y-1)}\big)\\ &\quad+b(1-qb)(1-q)q^{H(x,y)}\big(q^{H(x,y)}-q^{H(x-1,y)}\big)\\ &\quad-b(1-b)(1-q)q^{H(x,y)}\big(q^{H(x,y)}-q^{H(x,y-1)}\big)\big].\end{aligned}\tag{109}$$

We split (109) into two parts: the leading contribution and vanishing terms. The former is given by the third and fourth lines with $L\to\infty$ approximations $q^H\approx 1$

and $q^{H(x,y)} - q^{H(x-1,y)} \approx \ln(q)(H(x,y) - H(x-1,y))$:

$$\begin{aligned} & b(1-qb)(1-q)\ln(q)\sum_{x=1}^{LX}\sum_{y=1}^{LY}\mathcal{R}^d(LX,LY;x,y)^2 \\ & \quad \times \mathbb{E}\big[H(x,y) - H(x-1,y)\big] \\ & \quad - b(1-b)(1-q)\ln(q)\sum_{x=1}^{LX}\sum_{y=1}^{LY}\mathcal{R}^d(LX,LY;x,y)^2 \\ & \quad \times \mathbb{E}\big[H(x,y) - H(x,y-1)\big]. \end{aligned} \tag{110}$$

We sum by parts in (110) and compute the limit $L \to \infty$. For the first sum, we get

$$\begin{aligned} & b(1-qb)(1-q)\ln(q) \\ & \quad \times \Bigg[\sum_{x=1}^{LX}\sum_{y=1}^{LY}[\mathcal{R}^d(LX,LY;x,y)^2 \\ & \quad - \mathcal{R}^d(LX,LY;x+1,y)^2]\mathbb{E}H(x,y) \\ & \quad + \sum_{y=1}^{LY}\mathcal{R}^d(LX,LY;LX+1,y)^2\mathbb{E}H[LX,y] \\ & \quad - \sum_{y=1}^{LY}\mathcal{R}^d(LX,LY;1,y)^2\mathbb{E}H(0,y)\Bigg]. \end{aligned} \tag{111}$$

The explicit formula (45) implies that $L(\mathcal{R}^d(LX,LY;Lx,Ly)^2 - \mathcal{R}^d(LX,LY;Lx+1,Ly)^2) \to -\frac{\partial}{\partial x}\mathcal{R}^2(X,Y;x,y)$ as $L \to \infty$. Combining with (102), we obtain the $L \to \infty$ asymptotics of (111):

$$\begin{aligned} & L^{-1-\delta}\beta_2(\beta_2-\beta_1)^2\bigg[\int_0^X\int_0^Y\Big(-\frac{\partial}{\partial x}\mathcal{R}^2(X,Y;x,y)\Big)\mathbf{h}(x,y)\,dx\,dy \\ & \quad + \int_0^Y\mathcal{R}(X,Y;X,y)^2\mathbf{h}[X,y]\,dy - \int_0^Y\mathcal{R}(X,Y;0,y)^2\mathbf{h}(0,y)\,dy\bigg]. \end{aligned} \tag{112}$$

We further integrate by parts in (112) and do the same computation for the second sum in (110). The final result is

$$L^{-1-\delta}(\beta_2-\beta_1)^2\int_0^X\int_0^Y\mathcal{R}^2(X,Y;x,y)\big(\beta_2\mathbf{h}_x(x,y) - \beta_1\mathbf{h}_y(x,y)\big)\,dx\,dy. \tag{113}$$

Note that this is precisely the variance of $(\beta_1-\beta_2)\phi(X,Y)$, when we use Theorem 4.4 to solve (101).

The next step is to show that the remaining terms in (109) indeed do not contribute to the leading asymptotic behavior. We start from the second line in (109).

Note that $(q^{H(x,y)} - q^{H(x-1,y)})(q^{H(x,y)} - q^{H(x,y-1)}) \le 0$ and $\mathcal{R}^d$ is uniformly bounded as $L \to \infty$ (because it converges to $\mathcal{R}$). Thus, the absolute value of the first line in (109) is bounded by (here C is a positive constant)

$$\frac{C}{L}\mathbb{E}\sum_{x=1}^{LX}\sum_{y=1}^{LY}\big(q^{H(x-1,y)} - q^{H(x,y)}\big)\big(q^{H(x,y)} - q^{H(x,y-1)}\big). \tag{114}$$

Note that the (x, y)-summand is nonzero if and only if both $H(x-1, y) = H(x, y) + 1$ and $H(x, y-1) = H(x, y)$. In other words, this happens if the vertex at (x, y) has type *II* (cf. Figure 3). We conclude that (114) is bounded from above by

$$\frac{C'}{L^3}\mathbb{E}\big(\text{number of vertices of type } II \text{ inside } [1, LX] \times [1, LY]\big). \tag{115}$$

We proceed to bound this expectation. For that, let us first bound the expected number of vertices of types *V* and *VI* (corners). Let us denote the latter number by $\mathcal{N}$. Note that we have $O(L^{1-\delta})$ paths entering into $[1, LX] \times [1, LY]$ from the left or from below. Each path has $O(L^{-1})$ vertices, and at each of these vertices with probability at most $1 - b_1$ or $1 - b_2$ a corner might occur. We conclude that there are $O(1)$ corners along each path. It follows that $\mathbb{E}\mathcal{N} = O(L^{1-\delta})$ and $\mathbb{E}\mathcal{N}^2 = O(L^{2-2\delta})$. Next, note that each vertex of type *II* must belong to a column (vertical line of fixed x-coordinate) in which either a path enters into the quadrant from below or there is a corner in this column. For the same reason, each vertex of type *II* must belong to a row with similar properties. Since the number of both such rows and columns is $O(L^{1-\delta})$, we conclude that the number of vertices of type *II* is $O(L^{1-\delta} \cdot L^{1-\delta})$. Plugging into (115), we get

$$\frac{C'}{L^3} O\big(L^{1-\delta} \cdot L^{1-\delta}\big) = O\big(L^{-1-2\delta}\big),$$

which is of lower order than the leading term of (109). The justification of the fact that the remainder terms that were left out when passing from (109) to (110) is straightforward and we omit it.

We have computed the asymptotic variance of (108) and now proceed to showing the asymptotic Gaussianity. Let us linearly order the integer points inside the rectangle $[1, LX] \times [1, LY]$ as follows: (1, 1), (2, 1), (1, 2), (3, 1), (2, 2), (1, 3), (4, 1), (3, 2), (2, 3), (1, 4), ..., that is, we sequentially trace the diagonals $x + y = \text{const}$. Theorem 3.1 implies that then $\mathcal{R}^d(LX, LY; x, y)\xi(x, y)$ is then a martingale difference in (x, y), and we can apply the martingale central limit theorem; see, for example, [42], Section 3. There are two conditions to check:

1. The conditional variance, which by Theorem 3.1 is given by (the expression below differs from (109) by the absence of the expectation)

$$\sum_{x=1}^{LX}\sum_{y=1}^{LY}\mathcal{R}^d(LX, LY; x, y)^2$$

$$
\begin{aligned}
&\times \big[\big(qb(1-b)+b(1-qb)\big)\big(q^{H(x,y)}-q^{H(x-1,y)}\big)\big(q^{H(x,y)}-q^{H(x,y-1)}\big)\\
&+b(1-qb)(1-q)q^{H(x,y)}\big(q^{H(x,y)}-q^{H(x-1,y)}\big)\\
&-b(1-b)(1-q)q^{H(x,y)}\big(q^{H(x,y)}-q^{H(x,y-1)}\big)\big],
\end{aligned} \tag{116}
$$

should have the same $L\to\infty$ behavior as the unconditional variance (109), in the sense that the ratio tends to 1 in probability.

2. The Lindeberg condition should hold, which in our setting reads

$$
\lim_{L\to\infty}\sum_{x=1}^{LX}\sum_{y=1}^{LY}\mathbb{E}\big[\xi^2(x,y)L^{1+\delta}I_{\xi^2(x,y)L^{1+\delta}>\varepsilon}\big]=0 \quad \text{for each } \varepsilon>0. \tag{117}
$$

For the first condition, note that since we already know the decay of variance in (109), we can infer that $L^{1-\delta}H(Lx,Ly)\to \mathbf{h}(x,y)$ in probability. Since H is a monotone function in each of its variables, the one-point convergence further implies the convergence to $\mathbf{h}$ as a continuous function of two variables in the supremum norm. Then the same argument as for (109) goes through and we obtain the same asymptotics (113) for (116) as for (109).

For the Lindeberg condition, note that by its definition (31), $|\xi(x,y)|$ is uniformly bounded by C/L for a deterministic constant C. Thus, the indicator $I_{\xi^2(x,y)L^{1+\delta}>\varepsilon}$ becomes empty as $L\to\infty$, and the expression (117) vanishes for large L.

The asymptotic Gaussianity follows, and we have thus shown the following convergence in finite-dimensional distributions:

$$
\lim_{L\to\infty} L^{\frac{1+\delta}{2}}\big[q^{H(LX,LY)}-\mathbb{E}q^{H(LX,LY)}\big]=(\beta_1-\beta_2)\phi(X,Y). \tag{118}
$$

It remains to deduce the same convergence for centered and rescaled $H(LX,LY)$. For that, we write

$$
\begin{aligned}
q^{H(LX,LY)} &= q^{\mathbb{E}H(LX,LY)}q^{H(LX,LY)-\mathbb{E}H(LX,LY)}\\
&= q^{\mathbb{E}H(LX,LY)}\sum_{n=0}^{\infty}\frac{[\ln(\mathfrak{q})(H(LX,LY)-\mathbb{E}H(LX,LY))]^n}{n!L^n}.
\end{aligned} \tag{119}
$$

Since $\ln(\mathfrak{q})H(LX,LY)/L$ is bounded by a deterministic constant, the series in (119) is uniformly convergent, and $q^{H(LX,LY)}-\mathbb{E}q^{H(LX,LY)}$ is the centered version of the same series:

$$
\begin{aligned}
&q^{\mathbb{E}H(LX,LY)}\sum_{n=1}^{\infty}\bigg(\frac{[\ln(\mathfrak{q})(H(LX,LY)-\mathbb{E}H(LX,LY))]^n}{n!L^n}\\
&\qquad -\frac{\mathbb{E}[\ln(\mathfrak{q})(H(LX,LY)-\mathbb{E}H(LX,LY))]^n}{n!L^n}\bigg).
\end{aligned} \tag{120}
$$

As $L \to \infty$, the prefactor $q^{\mathbb{E}H(LX,LY)}$ tends to 1, the first term in the series is

$$\frac{\ln(\mathfrak{q})}{L}\big(H(LX,LY) - \mathbb{E}H(LX,LY)\big),$$

and the following terms are of lower orders. Since $\ln(\mathfrak{q}) = \beta_1 - \beta_2$, (118) now implies

$$\lim_{L\to\infty} L^{\frac{1+\delta}{2}} \frac{\beta_1 - \beta_2}{L}\big(H(LX,LY) - \mathbb{E}H(LX,LY)\big) = (\beta_1 - \beta_2)\phi(X,Y),$$

and the proof of Theorem 7.1 is complete.

APPENDIX B: THEOREM 6.1 THROUGH A VARIATIONAL PRINCIPLE AND CONTOUR INTEGRALS

In this section, we provide an alternative arguments toward the validity of Theorem 6.1. This is not a rigorous proof, only heuristics.

This approach to Theorem 6.1 was inspired by [8], Appendix. In a sense, we develop (nonrigorously) a version of the local variational principle for the stochastic six-vertex model in the limit regime (4). It would be interesting to see whether this variational principle can be applied to other situations. For the computations, we rely on contour integral formulas of [2].

We start by considering another integrable case of boundary conditions for the stochastic six-vertex model that generalizes domain wall boundary conditions of Section 2.

At each point of the y-axis we flip an independent coin. It comes heads with probability p_1, and in such a case we place a path entering from the left at this point. Otherwise, there is no path. Similarly, for each point of the x-axis we flip a coin which comes heads with probability p_2 to create paths entering from the bottom. [2] develops proves a multiple contour integral formula for the joint moments of q^H in this situation, generalizing the $\alpha = 0$ case of Theorem 2.6. The formulas are quite similar and only differ by simple rational factors.

In particular, [2], (3.13), (3.19), yields

$$\begin{aligned}
&\mathbb{E}q^{n\cdot H(x,y)} \\
&\quad= (\rho_1^{-1}\rho_2\mathfrak{s}^{-1}q^{-n};q)_n \frac{q^{n(n-1)/2}}{(2\pi\mathbf{i})^n}\oint\cdots\oint \prod_{1\le i<j\le n}\frac{z_i - z_j}{z_i - qz_j} \\
&\qquad\times \prod_{i=1}^n\Big[\Big(\frac{1+q^{-1}\frac{1-b}{1-qb}z_i}{1+\frac{1-b}{1-qb}z_i}\Big)^{x-1}\Big(\frac{1+z_i}{1+q^{-1}z_i}\Big)^y \\
&\qquad\times \frac{1}{(1-q^{-1}\rho_1^{-1}z_i)(z_i - \rho_2\frac{1-qb}{1-b})}\,dz_i\Big],
\end{aligned} \tag{121}$$

where $n \geq 1$, $\rho_i = \frac{p_i}{1-p_i}$, and the contours have two parts: the first ones are *nested* around $\{\frac{1-qb}{1-b}\rho_2\}$, and the second ones all coincide with a tiny circle around $-q$. The contours avoid singularities at $-\frac{1-qb}{1-b}$ and at $\rho_1 q$. In [2], the formula (121) is proven in the case $\rho_1^{-1}\rho_2\mathfrak{s}^{-1}q^{-n} < 1$; for other values of parameters, one needs to make an analytic continuation in ρ_1, ρ_2 of both sides in (121).

The following statement is a simple corollary of (121), extending Theorem 2.1 and matching the computations of Section 5.2.

PROPOSITION B.1. *In the regime* (4), *with the Bernoulli boundary conditions as described above,* $\frac{1}{L}H(Lx, Ly)$ *converges to* $\mathbf{h}(x, y)$ *given by*

$$\begin{aligned} \mathfrak{q}^{\mathbf{h}(x,y)} = {} & \frac{1}{2\pi\mathbf{i}} \oint_{-1} \exp\Bigl(\ln(\mathfrak{q})\Bigl(-x\frac{\mathfrak{s}z}{1+\mathfrak{s}z} + y\frac{z}{1+z}\Bigr)\Bigr) \\ & \times \Bigl(\frac{1}{\rho_1 - z} + \frac{1}{z - \rho_2\mathfrak{s}^{-1}}\Bigr)\,dz \\ & + \exp\Bigl(\ln(\mathfrak{q})\Bigl(-x\frac{\rho_2}{1+\rho_2} + y\frac{\rho_2\mathfrak{s}^{-1}}{1+\rho_2\mathfrak{s}^{-1}}\Bigr)\Bigr), \end{aligned} \tag{122}$$

with positively oriented integration contour that encircles only the singularity at $z = -1$.

REMARK B.2. When $\rho_1 = \rho_2\mathfrak{s}^{-1}$, the distribution of the system is translationally invariant; see [2]. This matches (122) turning into $\mathfrak{q}^{\mathbf{h}(x,y)} = \mathfrak{q}^{-xp_2+yp_1}$.

An important quantity for us is the second mixed derivative of (122) at 0:

$$M^{\varepsilon}(x, y) := \mathfrak{q}^{\mathbf{h}(\varepsilon x,\varepsilon y)} - \mathfrak{q}^{\mathbf{h}(\varepsilon x,0)} - \mathfrak{q}^{\mathbf{h}(0,\varepsilon y)} + \mathfrak{q}^{\mathbf{h}(0,0)}. \tag{123}$$

Direct computation shows that, as $\varepsilon \to 0$,

$$\begin{aligned} M^{\varepsilon}(x, y) &= \varepsilon^2 xy \ln^2(\mathfrak{q})\frac{p_1\mathfrak{s} - p_2}{1-\mathfrak{s}} + o(\varepsilon^2) \\ &= \varepsilon^2 xy(\beta_2 - \beta_1)(p_1\beta_1 - p_2\beta_2) + o(\varepsilon^2). \end{aligned} \tag{124}$$

The computation (121) admits an extension to joint q-moments for several points (x, y), that lie on the same vertical or same horizontal line, similar to Theorem 2.6. We can even reach the collections of points on more general monotone paths:

$$(x_1, y_1), (x_2, y_2), \dots, (x_k, y_k) : x_1 \geq x_2 \geq \cdots \geq x_k,\ y_1 \leq y_2 \leq \cdots \leq y_k; \tag{125}$$

for the domain wall boundary conditions this was done in [11], and here the situation is analogous.

It is very plausible that arguing similarly to the proof of CLT in Section 2, one can reach the following statement.

CLAIM B.3. *For the stochastic six-vertex model with Bernoulli boundary conditions as described above, as $L \to \infty$ in the regime* (4), $L^{1/2}(q^{H(Lx,Ly)} - \mathbb{E}q^{H(Lx,Ly)})$ *converges to a Gaussian random variable* (*jointly over monotone sections* (125)) *with variance given for* $x_1 \geq x_2$, $y_1 \leq y_2$ *by*

$$\begin{aligned}
&\lim_{L\to\infty} L\big(\mathbb{E}(q^{H(Lx_1,Ly)}q^{H(Lx_2,Ly)} - \mathbb{E}q^{H(Lx_1,Ly_1)}\mathbb{E}q^{H(Lx_2,Ly_2)})\big) \\
&\quad= \frac{\ln(\mathrm{q})}{(2\pi\mathbf{i})^2}\oint\oint \frac{z_1\rho_1 - z_2\rho_2\mathfrak{s}^{-1}}{(z_1-z_2)(\rho_1-\rho_2\mathfrak{s}^{-1})} \\
&\qquad\times\prod_{i=1}^{2}\Big[\exp\Big(\ln(\mathrm{q})\Big(-x_i\frac{\mathfrak{s}z_i}{1+\mathfrak{s}z_i} + y_i\frac{z_i}{1+z_i}\Big)\Big) \\
&\qquad\times\Big(\frac{1}{\rho_1 - z_i} + \frac{1}{z_i - \rho_2\mathfrak{s}^{-1}}\Big)dz_i\Big],
\end{aligned} \tag{126}$$

where the integration goes in positive direction around the singularities at -1 *and at* $\rho_2\mathfrak{s}^{-1}$, *and* z_1 *is inside* z_2.

REMARK B.4. The right-hand side of (126) depends on ρ_1, ρ_2 in an analytic way; in order to continue through the line $\rho_1 = \rho_2\mathfrak{s}^{-1}$, one should split z_1 and z_2 integrals into two parts: enclosing -1 and enclosing $\rho_2\mathfrak{s}^{-1}$. The latter part can then be explicitly computed.

Let $\tilde{h}(x,y)$ denote the limiting Gaussian field of Claim B.3. We are interested in the following mixed difference:

$$D^{\varepsilon}(x,y) := \tilde{h}(\varepsilon x, \varepsilon y) + \tilde{h}(0,0) - \tilde{h}(\varepsilon x, 0) - \tilde{h}(0, \varepsilon y). \tag{127}$$

Note that $\tilde{h}(0,0) = 0$, but we still add it to the formula in order to emphasize the structure. Claim B.3 implies that $D^{\varepsilon}(x,y)$ is Gaussian, and we would like to find its variance as $\varepsilon \to 0$. We compute

$$\begin{aligned}
&\mathrm{Var}\big(D^{\varepsilon}(x,y)\big) \\
&\quad= \mathrm{Cov}\big(\tilde{h}(\varepsilon x,\varepsilon y), \tilde{h}(\varepsilon x,\varepsilon y)\big) \\
&\qquad+ \mathrm{Cov}\big(\tilde{h}(\varepsilon x,0), \tilde{h}(\varepsilon x,0)\big) + \mathrm{Cov}\big(\tilde{h}(0,\varepsilon y), \tilde{h}(0,\varepsilon y)\big) \\
&\qquad- 2\,\mathrm{Cov}\big(\tilde{h}(\varepsilon x,\varepsilon y), \tilde{h}(\varepsilon x,0)\big) - 2\,\mathrm{Cov}\big(\tilde{h}(\varepsilon x,\varepsilon y), \tilde{h}(0,\varepsilon y)\big) \\
&\qquad+ 2\,\mathrm{Cov}\big(\tilde{h}(\varepsilon x,0), \tilde{h}(0,\varepsilon y)\big),
\end{aligned} \tag{128}$$

where the last term vanishes, as the boundary values are independent. We use the expression of Claim B.3 for each term of (128), expand the exponentials in series in ε, and compute the integrals as residues. Simplifying the result and expressing it in terms of p_1, p_2 we get

$$\begin{aligned}
&\mathrm{Var}\big[D^\varepsilon(x,y)\big]\\
&\quad= -\varepsilon^2 xy \ln^3(\mathfrak{q}) \frac{-p_1p_2(\mathfrak{s}+1)+p_1\mathfrak{s}+p_2}{1-\mathfrak{s}} + o(\varepsilon^2)\\
&\quad= \varepsilon^2 xy(\beta_2-\beta_1)^2\big(-p_1p_2(\beta_1+\beta_2)+p_1\beta_1+p_2\beta_2\big)+o(\varepsilon^2).
\end{aligned} \tag{129}$$

Note that the individual terms in the definition of $D^\varepsilon(x,y)$ have much greater variance. For instance, $\mathrm{Var}\,\tilde{h}(\varepsilon x,0)=\varepsilon x p_2(1-p_2)$ due to the conventional CLT for sums of independent Bernoulli random variables. However, mixed difference leads to cancelations, and (129) has variance of order ε^2 rather than ε.

HEURISTIC PROOF OF THEOREM 6.1. Fix small $\varepsilon>0$ and consider the values of the height function H at points $(\varepsilon i,\varepsilon j)$, $i,j=1,2,\dots$ inside a fixed $[0,A]\times[0,B]$ rectangle.

We would like to compute the conditional distribution of $q^{H(\varepsilon L(i+1),\varepsilon L(j+1))}$ given $q^{H(\varepsilon Li,\varepsilon Lj)}$, $q^{H(\varepsilon L(i+1),\varepsilon Lj)}$, $q^{H(\varepsilon Li,\varepsilon L(j+1))}$.

At this moment, we will make a nonrigorous step, approximating the system in an $\varepsilon L\times\varepsilon L$ square by the system with Bernoulli boundary conditions as in Proposition B.1, Claim B.3 in a similarly sized square. Therefore, we say that when ε is small and L is large, the horizontal lines crossing the vertical segment between points $(\varepsilon Li,\varepsilon Lj)$ and $(\varepsilon Li,\varepsilon L(j+1))$ become Bernoulli-distributed with parameter

$$p_1 \approx \frac{H(\varepsilon Li,\varepsilon L(j+1))-H(\varepsilon Li,\varepsilon Lj)}{\varepsilon L}.$$

The vertical lines crossing the horizontal segment between points $(\varepsilon Li,\varepsilon Lj)$ and $(\varepsilon L(i+1),\varepsilon L(j))$ also become Bernoulli-distributed with parameter

$$p_2 \approx \frac{H(\varepsilon Li,\varepsilon Lj))-H(\varepsilon L(i+1),\varepsilon Lj)}{\varepsilon L}.$$

At this point, we can use Claim B.3, which will give us the conditional distribution as a Gaussian law. Shortening the notation as $h_{ij}=H(\varepsilon Li,\varepsilon Lj)$, we write

$$\begin{aligned}
&\mathrm{Prob}\big(q^{h_{i+1,j+1}}\mid q^{h_{i,j}},q^{h_{i+1,j}},q^{h_{i,j+1}}\big)\\
&\approx \frac{1}{\sqrt{2\pi\varepsilon^2 LV[p_2,p_1]}}\\
&\quad\times\exp\bigg(-\frac{(q^{h_{i+1,j+1}}-q^{h_{i+1,j}}-q^{h_{i,j+1}}+q^{h_{i,j}}-L\varepsilon^2M(p_1,p_2))^2}{2\varepsilon^2LV[p_1,p_2]}\bigg),
\end{aligned}\tag{130}$$

where $\varepsilon^2M(p_1,p_2)$ is $\mathfrak{q}^{\mathbf{h}}$ multiplied by the leading $\varepsilon\to0$ term of the expression (124) with $x=y=1$, and $\varepsilon^2V[p_1,p_2]$ is $\mathfrak{q}^{2\mathbf{h}}$ multiplied by the leading $\varepsilon\to0$

term of the expression (129) with $x = y = 1$. The multiplication by $\mathfrak{q}^{\mathbf{h}}$ and $\mathfrak{q}^{2\mathbf{h}}$ appears because of the height function at the origin was zero in Proposition B.1 and Claim B.3, while we need the value h_{ij} here.

At this point, we can multiply (130) over all i, j to get the joint law of $h_{i,j}$, $i, j = 1, 2, \dots$. Implicitly, we use the Markovian structure of the stochastic six-vertex model here.

Now let us analyze various parts of (130). Recall that as $L \to \infty$, $q^{H(Lx,Ly)}$ approximates a smooth profile $\mathfrak{q}^{\mathbf{h}}(x, y)$ plus $\frac{1}{\sqrt{L}}$ multiplied by the fluctuation field $\phi(x, y)$ as in Theorem 6.1. Then we have

$$p_1 \approx \frac{\partial}{\partial y}\frac{1}{L}H(Lx, Ly) \approx \frac{\mathfrak{q}^{\mathbf{h}}_y + L^{-1/2}\phi_y}{\ln(\mathfrak{q})\mathfrak{q}^{\mathbf{h}}},$$

$$p_2 \approx -\frac{\partial}{\partial x}\frac{1}{L}H(Lx, Ly) \approx -\frac{\mathfrak{q}^{\mathbf{h}}_x + L^{-1/2}\phi_x}{\ln(\mathfrak{q})\mathfrak{q}^{\mathbf{h}}},$$

$$q^{h_{i+1,j+1}} - q^{h_{i+1,j}} - q^{h_{i,j+1}} + q^{h_{i,j}} \approx \mathfrak{q}^{\mathbf{h}}_{xy}\varepsilon^2 L + \phi_{xy}(\varepsilon i, \varepsilon j)\varepsilon^2 L^{1/2}.$$

Therefore, plugging in the expression for $M[p_1, p_2]$, the joint law of all $h_{i,j}$ can be approximated as

$$\prod_{i,j}\left(2\pi\varepsilon^2 L V\left[\frac{\mathfrak{q}^{\mathbf{h}}_y}{\ln(\mathfrak{q})\mathfrak{q}^{\mathbf{h}}}, -\frac{\mathfrak{q}^{\mathbf{h}}_x}{\ln(\mathfrak{q})\mathfrak{q}^{\mathbf{h}}}\right]\right)^{-1/2} \times \exp\left(-L\varepsilon^2\frac{(\mathfrak{q}^{\mathbf{h}}_{xy} + \beta_1\mathfrak{q}^{\mathbf{h}}_y + \beta_2\mathfrak{q}^{\mathbf{h}}_x + L^{-1/2}(\phi_{xy} + \beta_1\mathfrak{q}^{\mathbf{h}}_y + \beta_2\mathfrak{q}^{\mathbf{h}}_x)^2}{2V[\frac{\mathfrak{q}^{\mathbf{h}}_y}{\ln(\mathfrak{q})\mathfrak{q}^{\mathbf{h}}}, -\frac{\mathfrak{q}^{\mathbf{h}}_x}{\ln(\mathfrak{q})\mathfrak{q}^{\mathbf{h}}}]}\right), \tag{131}$$

where in (i, j)th term all functions are evaluated at the point $(x, y) = (\varepsilon i, \varepsilon j)$.

Theorem 5.1 says that $\mathfrak{q}^{\mathbf{h}}_{xy} + \beta_1\mathfrak{q}^{\mathbf{h}}_y + \beta_2\mathfrak{q}^{\mathbf{h}}_x$ in (131) vanishes.[6] Plugging in the expression for $V[\cdot, \cdot]$, we further approximate the joint law of all $h_{i,j}$ by

$$\prod_{i,j}\frac{1}{\sqrt{2\pi\varepsilon^2 L(\mathfrak{q}^{\mathbf{h}}_y\mathfrak{q}^{\mathbf{h}}_x(\beta_1+\beta_2) + \mathfrak{q}^{\mathbf{h}}_x\mathfrak{q}^{\mathbf{h}}\beta_2(\beta_2-\beta_1) - \mathfrak{q}^{\mathbf{h}}_y\mathfrak{q}^{\mathbf{h}}\beta_1(\beta_2-\beta_1))}} \times \exp\left(-\varepsilon^2\frac{(\phi_{xy} + \beta_1\mathfrak{q}^{\mathbf{h}}_y + \beta_2\mathfrak{q}^{\mathbf{h}}_x)^2}{2(\mathfrak{q}^{\mathbf{h}}_y\mathfrak{q}^{\mathbf{h}}_x(\beta_1+\beta_2) + \mathfrak{q}^{\mathbf{h}}_x\mathfrak{q}^{\mathbf{h}}\beta_2(\beta_2-\beta_1) - \mathfrak{q}^{\mathbf{h}}_y\mathfrak{q}^{\mathbf{h}}\beta_1(\beta_2-\beta_1))}\right). \tag{132}$$

Note that informally the second line in (132) approximates as $\varepsilon \to 0$ the exponential of a double integral, which shows that the scalings are chosen in the correct way. On the other hand, it matches Theorem 6.1. Indeed, the numerator in the exponential is the left-hand side of (82), and the denominator is the same as the

[6] Alternatively, one can use the leading exponential part of (131) to *show* that $\mathfrak{q}^{\mathbf{h}}_{xy} + \beta_1\mathfrak{q}^{\mathbf{h}}_y + \beta_2\mathfrak{q}^{\mathbf{h}}_x = 0$.

(squared) coefficient in the right-hand side. The noise in (82) is Gaussian, as is density in (132). Finally, the noise is white (uncorrelated), and (132) has the product structure over points of the plane manifesting the independence. □

Acknowledgments. We are very grateful to M. A. Borodin for bringing the telegraph equation and its treatment in [28] to our attention. We would like to thank I. Corwin and H. Spohn for very helpful discussions, P. Diaconis for pointing us to the lectures [55], M. Wheeler for the discussions which eventually led us to the discovery of the four-point relation, H. Shen and L.-C. Tsai for telling us about their work [61] and three referees for the careful proofreading of the manuscript.

REFERENCES

[1] AGGARWAL, A. (2017). Convergence of the stochastic six-vertex model to the ASEP: Stochastic six-vertex model and ASEP. *Math. Phys. Anal. Geom.* **20** Art. 3. MR3589552

[2] AGGARWAL, A. (2018). Current fluctuations of the stationary ASEP and six-vertex model. *Duke Math. J.* **167** 269–384. MR3754630

[3] AGGARWAL, A. (2018). Dynamical stochastic higher spin vertex models. *Selecta Math.* (*N.S.*) **24** 2659–2735. MR3816514

[4] AMIR, G., CORWIN, I. and QUASTEL, J. (2011). Probability distribution of the free energy of the continuum directed random polymer in $1+1$ dimensions. *Comm. Pure Appl. Math.* **64** 466–537. MR2796514

[5] BARRAQUAND, G., BORODIN, A., CORWIN, I. and WHEELER, M. Stochastic six-vertex model in a half-quadrant and half-line open ASEP. Available at arXiv:1704.04309.

[6] BAXTER, R. J. (2007). *Exactly Solved Models in Statistical Mechanics*. Dover.

[7] BERTINI, L. and GIACOMIN, G. (1997). Stochastic Burgers and KPZ equations from particle systems. *Comm. Math. Phys.* **183** 571–607. MR1462228

[8] BODINEAU, T. and DERRIDA, B. (2005). Distribution of current in nonequilibrium diffusive systems and phase transitions. *Phys. Rev. E* (3) **72** 066110, 8. MR2203647

[9] BORODIN, A. Symmetric elliptic functions, IRF models, and dynamic exclusion processes. Available at arXiv:1701.05239.

[10] BORODIN, A. (2018). Stochastic higher spin six vertex model and Macdonald measures. *J. Math. Phys.* **59** 023301, 17. MR3760963

[11] BORODIN, A., BUFETOV, A. and WHEELER, M. Between the stochastic six vertex model and Hall–Littlewood processes. Available at arXiv:1611.09486.

[12] BORODIN, A., CORWIN, I. and GORIN, V. (2016). Stochastic six-vertex model. *Duke Math. J.* **165** 563–624. MR3466163

[13] BORODIN, A. and GORIN, V. (2015). General β-Jacobi corners process and the Gaussian free field. *Comm. Pure Appl. Math.* **68** 1774–1844. MR3385342

[14] BORODIN, A. and OLSHANSKI, G. (2017). The ASEP and determinantal point processes. *Comm. Math. Phys.* **353** 853–903. MR3649488

[15] BORODIN, A. and PETROV, L. (2017). Integrable probability: Stochastic vertex models and symmetric functions. In *Stochastic Processes and Random Matrices* 26–131. Oxford Univ. Press, Oxford. MR3728714

[16] BORODIN, A. and PETROV, L. (2018). Higher spin six vertex model and symmetric rational functions. *Selecta Math.* (*N.S.*) **24** 751–874. MR3782413

[17] CABAÑA, E. (1970). The vibrating string forced by white noise. *Z. Wahrsch. Verw. Gebiete* **15** 111–130. MR0279909

[18] CAIROLI, R. (1972). Sur une équation différentielle stochastique. *C. R. Acad. Sci. Paris Sér. A-B* **274** A1739–A1742. MR0301796

[19] CARMONA, R. and NUALART, D. (1988). Random nonlinear wave equations: Smoothness of the solutions. *Probab. Theory Related Fields* **79** 469–508. MR0966173

[20] CARMONA, R. and NUALART, D. (1988). Random nonlinear wave equations: Propagation of singularities. *Ann. Probab.* **16** 730–751. MR0929075

[21] COHN, H., KENYON, R. and PROPP, J. (2001). A variational principle for domino tilings. *J. Amer. Math. Soc.* **14** 297–346. MR1815214

[22] CONUS, D. and DALANG, R. C. (2008). The non-linear stochastic wave equation in high dimensions. *Electron. J. Probab.* **13** 629–670. MR2399293

[23] CONUS, D., JOSEPH, M., KHOSHNEVISAN, D. and SHIU, S.-Y. (2013). Intermittency and chaos for a nonlinear stochastic wave equation in dimension 1. In *Malliavin Calculus and Stochastic Analysis* (F. Viens, J. Feng, Y. Hu and E. Nualart, eds.) *Springer Proc. Math. Stat.* **34** 251–279. Springer, New York. MR3070447

[24] CORWIN, I. (2012). The Kardar–Parisi–Zhang equation and universality class. *Random Matrices Theory Appl.* **1** 1130001, 76. MR2930377

[25] CORWIN, I., GHOSAL, P., SHEN, H. and TSAI, L.-C. Stochastic PDE limit of the six vertex model. Available at arXiv:1803.08120.

[26] CORWIN, I. and PETROV, L. (2016). Stochastic higher spin vertex models on the line. *Comm. Math. Phys.* **343** 651–700. MR3477349

[27] CORWIN, I. and TSAI, L.-C. (2017). KPZ equation limit of higher-spin exclusion processes. *Ann. Probab.* **45** 1771–1798. MR3650415

[28] COURANT, R. and HILBERT, D. (1989). *Methods of Mathematical Physics. Vol. II. Partial Differential Equations. Wiley Classics Library*. Wiley, New York. MR1013360

[29] DA PRATO, G. and ZABCZYK, J. (2014). *Stochastic Equations in Infinite Dimensions*, 2nd ed. *Encyclopedia of Mathematics and Its Applications* **152**. Cambridge Univ. Press, Cambridge. MR3236753

[30] DALANG, R., KHOSHNEVISAN, D., MUELLER, C., NUALART, D. and XIAO, Y. (2009). The stochastic wave equation. In *A Minicourse on Stochastic Partial Differential Equations* D. Khoshnevisan and F. Rassoul-Agha, eds.) *Lecture Notes in Math.* **1962**. Springer, Berlin. MR1500166

[31] DALANG, R. C. and FRANGOS, N. E. (1998). The stochastic wave equation in two spatial dimensions. *Ann. Probab.* **26** 187–212. MR1617046

[32] DALANG, R. C. and LÉVÊQUE, O. (2006). Second-order hyperbolic S.P.D.E.'s driven by homogeneous Gaussian noise on a hyperplane. *Trans. Amer. Math. Soc.* **358** 2123–2159. MR2197451

[33] DALANG, R. C. and MUELLER, C. (2009). Intermittency properties in a hyperbolic Anderson problem. *Ann. Inst. Henri Poincaré Probab. Stat.* **45** 1150–1164. MR2572169

[34] DALANG, R. C., MUELLER, C. and TRIBE, R. (2008). A Feynman–Kac-type formula for the deterministic and stochastic wave equations and other P.D.E.'s. *Trans. Amer. Math. Soc.* **360** 4681–4703. MR2403701

[35] DE MASI, A., PRESUTTI, E. and SCACCIATELLI, E. (1989). The weakly asymmetric simple exclusion process. *Ann. Inst. Henri Poincaré Probab. Stat.* **25** 1–38. MR0995290

[36] DITTRICH, P. and GÄRTNER, J. (1991). A central limit theorem for the weakly asymmetric simple exclusion process. *Math. Nachr.* **151** 75–93. MR1121199

[37] DUNKEL, J. and HÄNGGI, P. (2009). Relativistic Brownian motion. *Phys. Rep.* **471** 1–73. MR2503143

[38] ETHIER, S. N. and KURTZ, T. G. (1986). *Markov Processes: Characterization and Convergence*. Wiley, New York. MR0838085

[39] FUNAKI, T. (1983). Random motion of strings and related stochastic evolution equations. *Nagoya Math. J.* **89** 129–193. MR0692348

[40] GOLDSTEIN, S. (1951). On diffusion by discontinuous movements, and on the telegraph equation. *Quart. J. Mech. Appl. Math.* **4** 129–156. MR0047963

[41] GWA, L.-H. and SPOHN, H. (1992). Six-vertex model, roughened surfaces, and an asymmetric spin Hamiltonian. *Phys. Rev. Lett.* **68** 725–728. MR1147356

[42] HALL, P. and HEYDE, C. C. (1980). *Martingale Limit Theory and Its Application*. Academic Press, New York. MR0624435

[43] KAC, M. (1974). A stochastic model related to the telegrapher's equation. *Rocky Mountain J. Math.* **4** 497–509. MR0510166

[44] KARDAR, M., PARISI, G. and ZHANG, Y.-C. (1986). Dynamic scaling of growing interfaces. *Phys. Rev. Lett.* **56** 889–892.

[45] KENYON, R. and OKOUNKOV, A. (2007). Limit shapes and the complex Burgers equation. *Acta Math.* **199** 263–302. MR2358053

[46] KHOSHNEVISAN, D. and NUALART, E. (2008). Level sets of the stochastic wave equation driven by a symmetric Lévy noise. *Bernoulli* **14** 899–925. MR2543579

[47] KOVÁCS, M., LARSSON, S. and SAEDPANAH, F. (2010). Finite element approximation of the linear stochastic wave equation with additive noise. *SIAM J. Numer. Anal.* **48** 408–427. MR2646102

[48] MARTIN, A., PRIGARIN, S. M. and WINKLER, G. (2003). Exact and fast numerical algorithms for the stochastic wave equation. *Int. J. Comput. Math.* **80** 1535–1541. MR2031601

[49] MILLET, A. and SANZ-SOLÉ, M. (1999). A stochastic wave equation in two space dimension: Smoothness of the law. *Ann. Probab.* **27** 803–844. MR1698971

[50] MUELLER, C. (1997). Long time existence for the wave equation with a noise term. *Ann. Probab.* **25** 133–151. MR1428503

[51] NUALART, D. and TINDEL, S. (1997). Quasilinear stochastic hyperbolic differential equations with nondecreasing coefficient. *Potential Anal.* **7** 661–680. MR1473647

[52] ONDREJÁT, M. (2004). Existence of global mild and strong solutions to stochastic hyperbolic evolution equations driven by a spatially homogeneous Wiener process. *J. Evol. Equ.* **4** 169–191. MR2059301

[53] ORSINGHER, E. (1984). Damped vibrations excited by white noise. *Adv. in Appl. Probab.* **16** 562–584. MR0753514

[54] PALAMARCHUK, K. and RESHETIKHIN, N. The 6-vertex model with fixed boundary conditions. In *Proceedings of Solvay Workshop "Bethe Ansatz: 75 Years Later."* Available at arXiv:1010.5011.

[55] PINSKY, M. A. (1991). *Lectures on Random Evolution*. World Scientific, River Edge, NJ. MR1143780

[56] QUER-SARDANYONS, L. and SANZ-SOLÉ, M. (2006). Space semi-discretisations for a stochastic wave equation. *Potential Anal.* **24** 303–332. MR2224753

[57] RESHETIKHIN, N. Lectures on the integrability of the 6-vertex model. Available at arXiv:1010.5031.

[58] RESHETIKHIN, N. and SRIDHAR, A. (2018). Limit shapes of the stochastic six vertex model. *Comm. Math. Phys.* **363** 741–765. MR3858820

[59] ROVIRA, C. and SANZ-SOLÉ, M. (1996). The law of the solution to a nonlinear hyperbolic SPDE. *J. Theoret. Probab.* **9** 863–901. MR1419867

[60] SASAMOTO, T. and SPOHN, H. (2010). One-dimensional KPZ equation: An exact solution and its universality. *Phys. Rev. Lett.* **104** 230602.

[61] SHEN, H. and TSAI, L.-C. (2019). Stochastic telegraph equation limit for the stochastic six vertex model. *Proc. Amer. Math. Soc.* **147** 2685–2705. MR3951443

[62] WALSH, J. B. (1986). An introduction to stochastic partial differential equations. In *École D'été de Probabilités de Saint-Flour, XIV—1984*. *Lecture Notes in Math.* **1180** 265–439. Springer, Berlin. MR0876085

[63] WALSH, J. B. (2006). On numerical solutions of the stochastic wave equation. *Illinois J. Math.* **50** 991–1018. MR2247851

[64] WHEELER, M. (2016). Private communication.

DEPARTMENT OF MATHEMATICS
MASSACHUSETTS INSTITUTE OF TECHNOLOGY
77 MASSACHUSETTS AVENUE
CAMBRIDGE, MASSACHUSETTS 02139
USA
E-MAIL: borodin@math.mit.edu
vadicgor@gmail.com